Design of a Shoulder-Launched Anti-UAV Missile System

William Giffin [1], *Margaret Kilpatrick* [2], *Ted Vlady* [2], *Brenton J. Willier* [2], *Nicholas Brophy* [3],
Justin Dobbin [3], *Sofia Ocoro Giraldo* [3], *James Jutras* [3], *Nguyen Nguyen* [3], *Jose Romero* [3]
Aerospace Systems Design Laboratory
Georgia Institute of Technology, Atlanta, Georgia, 30332, United States

ISLAND

Intercepting Shoulder Launched
Armament for Neutralizing Drones

[1]Graduate Student, Georgia Tech, AIAA Student Member
[2]Graduate Research Assistant, Aerospace Systems Design Laboratory, AIAA Student Member
[3]Undergraduate Student, Georgia Tech, AIAA Student Member

Dr. Dimitri Mavris
Faculty Advisor

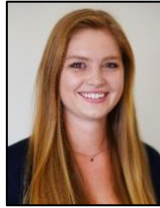Dr. Brad Robertson
Research Advisor

Dr. Adam Cox
Research Advisor

William Giffin
Structures
ASDL
AIAA #: 1230548

Margaret Kilpatrick
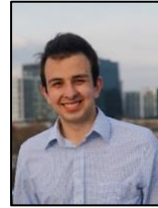Propulsion
ASDL
AIAA #: 1230547

Ted Vlady
Trajectory
ASDL
AIAA #: 921865

Brenton Willier
Aerodynamics
ASDL
AIAA #: 1218364

Nicholas Brophy
Propulsion
Undergraduate
AIAA #: 1230678

Justin Dobbin
Trajectory
Undergraduate
AIAA #: 923006

Sofia Ocoro Giraldo
Aerodynamics
Undergraduate
AIAA #: 1229424

James Jutras
Structures
Undergraduate
AIAA #: 1229357

Nguyen Nguyen
Trajectory
Undergraduate
AIAA #: 1146928

Jose Romero
Trajectory
Undergraduate
AIAA #: 1146929

Executive Summary

The ISLAND missile is a low-cost missile system that is specially designed to destroy Type 1 and Type 2 UAVs. It has a design range of 3.5 nautical miles and a design altitude of 5,000 feet. The system design, from the bottom up, was focused on user safety. Launch noise was minimized to a peak of 151 dBA, through the use of a custom first stage low noise rocket motor and through various noise mitigation techniques. ISLAND's noise levels are well below similar systems. The launch acceleration and the exhaust gases were mitigated through the use of an ejectable launch motor. The goal of the ISLAND missile system is to prevent asymmetric warfare, specifically against small UAV targets. The low cost seeker, simple materials, and commercial off the shelf ejectable launch motor allow ISLAND to meet this goal, with a acquisition price of only $35,000. Further orders of the ISLAND system can drive the price to below $25,000, similar in price to the Raytheon Coyote and over $10,000 cheaper than the Stinger. 3-D CAD renderings of the ISLAND missile and launcher are shown below.
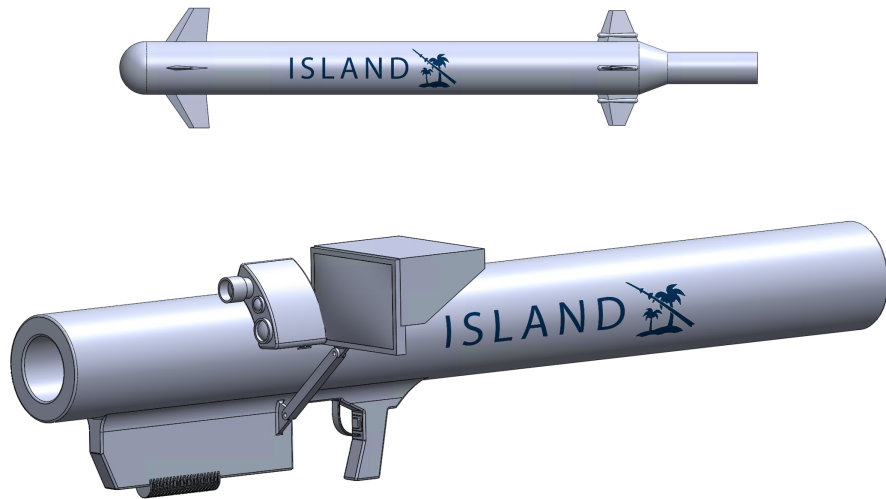
Table of Contents

List of Figures

List of Tables

1 Introduction

1.1 Project Introduction

This report details the final missile design of the Georgia Institute of Technology's Missile Design team for the 2020-2021 American Institute of Aeronautics and Astronautics (AIAA) Graduate Team Missile Systems Design Competition. Each year, AIAA hosts an intercollegiate Missile Systems Design Competition with a Request for Proposal (RFP) for a missile system that meets design requirements and has real-life applicability. For the 2020-2021 competition, the RFP calls for a shoulder-launched, anti-UAV missile system, capable of targeting, tracking, and destroying Type 1 and Type 2 UAVs. This report provides a detailed description and discussion of the design environment, the design process, and the final design for the ISLAND Missile.

1.2 Background and Existing Systems

As technology continues to advance, its accessibility in the commercial and military markets, both domestically and globally, continues to increase. One technology advancement to highlight is that of drones and other unmanned aerial vehicles (UAVs) in civilian, commercial, and military applications. Gaining popularity because of their low cost and versatility, both the commercial and military drone markets are expanding at a rapid rate [1]. As seen in Figure 1, there is a projected two-fold increase in the military spending on drones from 2018 to 2025. With the proliferation of these systems, however, comes security concerns in terms of air space security and defense.
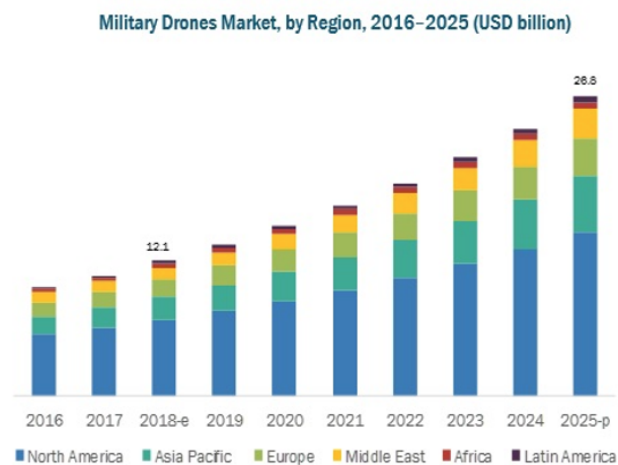
Figure 1: Military UAV Market Projections [1]

By definition, UAVs are considered to be any "powered, aerial vehicle that does not carry a human operator, uses aerodynamic forces to provide vehicle lift, can fly autonomously or be piloted remotely, can be expendable or recoverable, and can carry a lethal or non-lethal payload" [2]. As seen in Figure 2, UAVs are classified by their size, range, and speed. Type 1, 2, and 3 UAVs are typically smaller models with shorter ranges, can be easily acquired, and are available at low costs. Types 4 and 5 UAVs are less widespread, more susceptible to anti-aircraft weapons, similar in size to manned aircraft, and are capable of larger payloads and greater ranges.

The primary counter-UAV (c-UAV) capabilities, currently available in the U.S., are advanced air and missile defense systems. These systems are designed to protect against conventional attack aircraft, bombers, and ballistic missiles. Thus, current U.S. c-UAV capabilities are behind the curve, specifically in countering Type 1 and Type 2 low cost, small size, UAVs [3]. This gap in defensive capabilities for Type 1 and 2 UAVs is the motivation behind the design of this shoulder-launched, anti-UAV system.
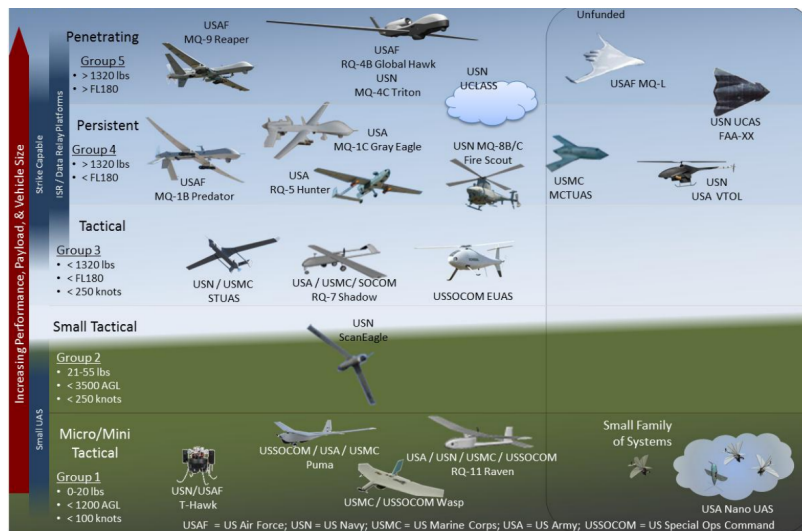
Figure 2: Current US UAV Defense Capabilities [4]

A shoulder-launched system allows for portability, providing a layer of defense to U.S. troops operating outside the protective range of advanced air and missile defense systems. The shoulder-launch system also reduces cost by decoupling the system from a vehicle or installation for operation. Low cost is an important feature to counter inexpensive commercially available drones.

Current c-UAV technologies exist in the form of current missiles, nets, directed energy, and cyber-takeovers. A brief summary of these technologies advantages and disadvantages can be seen below in Table 1.

Table 1: Pre-existing c-UAV Systems Advantages and Disadvantages

	Advantage	Disadvantage
Current Missiles	Proven against larger targets	Over-engineered
Net Entanglement	Low Cost	Slow, Low Accuracy
Directed Energy	Effective against swarms	Large battery capacity needed
Cyber Takeover	Low recurring cost	Not effective against autonomous vehicles

1.3   Target Characterization

Type 1 and 2 UAVs are small aerial systems with minimal weight and structure, typically with no hardening or armor, and with exposed and vulnerable propulsion and flight sensor components [5]. While these characteristics make the target more susceptible to damage, Type 1 and 2 UAVs are highly maneuverable, with vertical flight drones capable of extreme changes in altitude. Characteristics of Type 1 and 2 UAVs can be seen in Table 2, with examples depicted in Figure 3 and Figure 4.

Table 2: Type 1 and 2 UAV Characterization [5]

Category	Size	MGTW (lbs)	Max Operating Altitude (ft)	Max Airspeed (knots)	Max Maneuverability (g)
Type 1	Small	0-20	<1,200 AGL	< 100	1
Type 2	Medium	21-55	<3,500	<250	2

(a)   (b)
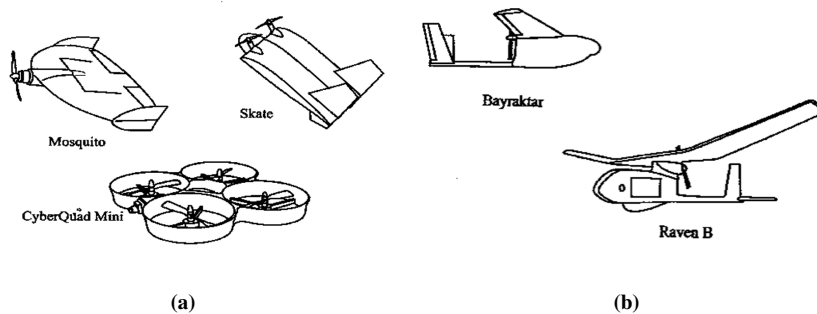
Figure 3: Small UAV's [5]
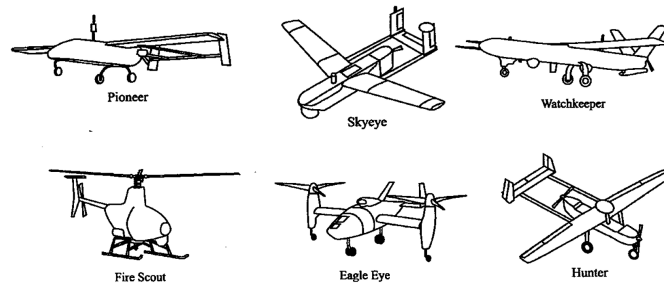
Figure 4: Medium UAV's [5]

2 Requirements

In the Systems Engineering V-model, the step following market analysis is requirement definition and concept of operations development [6]. This section will outline the team's interpretation of the explicit requirements, the derived requirements, and the proposed concept of operations for the ISLAND missile.

2.1 Explicit Requirements

The request for proposal, supplied by AIAA, outlines key requirements about the missile system performance, operations, and launch crew safety, as well as information on entry into service dates and production run estimates [7].

In terms of performance requirements, the missile system shall have a threshold range of 3.0 nautical miles and an objective range of 3.5 nautical miles. It shall have a threshold service ceiling of 3,000 ft above ground level and an objective service ceiling of 5,000 ft above ground level. The missile system, which includes one missile and one launcher, shall weigh no more than 40 pounds. Ten missiles and one launcher shall weigh no more than 125 pounds, split across three personnel, with each carrying no more than 50 pounds.

In terms of operations requirements, the system shall be capable of being used in a raid scenario where ten evenly spaced UAVs must be detected, acquired, targeted, and engaged over a time period of one hour. The design and development of the missile will begin in October 2022 and the initial operational capability (IOC) shall occur no later than December 2027. For production, a 10 year run with 200 missiles and 20 launchers per year is assumed. Fifteen additional missiles will be produced for developmental testing.

In terms of safety requirements, the system shall be able to be safely stored, transported and handled for ten years without maintenance. Furthermore, the launch acceleration shall be no more than 2g's, the warhead shall not be armed within 200 feet of the launch site, and the decibel noise level shall not exceed 120dB(A) within 100 ft of the launch location.

A summary of the explicit requirements can be found in Table 3, below.

Table 3: Explicit Requirements for ISLAND

	Threshold	Objective
Range (nmi)	3.0	3.5
Service Ceiling (ft)	3000	5000
Weight	40 lb. for 1 missile & 1 launcher 125 lb. for 10 missiles & 1 launcher	
Lifetime	10 years without maintenance	
Safety	Launch acceleration < 2g's Noise limit within 100 ft < 120dBA Warhead arming distance > 200 ft	
Production Run	200 missiles & 20 launchers per year for 10 years +15 missiles for development testing	
Entry Into Service	Development: October 2022 IOC: December 2027	

2.2   Derived Requirements

Additional requirements must be derived in order to complete a successful missile design and to satisfy the explicit requirements of the RFP. The derived requirements are grouped into the same three areas as the explicit requirements.

In terms of the derived performance requirements, the propulsion system shall be properly sized in order to meet the range and altitude requirements. The aerodynamics of the missile must provide sufficient lift and maneuverability performance to complete the mission. To successfully perform endgame maneuvers, the missile shall have about 3 times the maneuverability of its target [8]. Type 2 UAVs have a maneuverability no more than 2g's, thus the missile must have 6g's of maneuverability in the endgame. Lastly, the missile must have enough energy to execute endgame maneuvers. As a first order estimate, the missile shall have twice the specific energy as the target [9]. Assuming a Type 2 UAV traveling at 200 knots, the missile would need to be traveling at 283 knots in the endgame to meet this requirement.

In terms of the derived operations requirements, an operations model shall be developed to test the missile system against the raid scenario. Specifically, a reloading mechanism as well as specifics for powering the detection and tracking hardware shall be outlined. Because of the unique target, the missile seeker system shall be capable of detecting and targeting systems that have reduced visual, radar, and/or heat signatures. Additionally, the missile shall have a control system that is capable of successfully engaging UAVs that are highly maneuverable. Finally, the payload system must be capable of destroying or disabling the target and if it is determined that the payload is interchangeable, a robust payload exchange system must be designed.

Finally, in terms of the derived safety requirements, a warhead arming system must be implemented. Next, a "soft"

launch configuration shall be designed to limit the launch acceleration. Finally, additional sound mitigation must be implemented to meet the sound limits. Many of the configurations to reduce acceleration will assist in reducing noise, therefore these two safety requirements are highly coupled and sensitive to the final configuration.

A summary of the derived requirements can be found in Table 4.

Table 4: Derived Requirements for ISLAND

Performance Requirements	Missile shall have a properly sized propulsion system and aerodynamic surfaces
	Missile propulsion system shall be storable without maintenance
	Missile shall weigh less than 9.4 lbs, launcher shall weigh less than 30.6
	Missile shall have enough energy to engage the target in the endgame
	Missile shall travel at 283 knots and have 6g's of maneuverability in the endgame
Operations Requirements	A robust reload procedure must be designed
	Missile seeker and control configuration must be compatible with target type
	If needed, a robust payload exchange system must be designed
Safety Requirements	A smart arming system must be included
	A soft launch configuration is required to limit launch acceleration
	Sound mitigation must be considered

2.3   Concept of Operation

The ISLAND system will be deployed in a variety of situations and environments, both domestically and internationally. ISLAND can be used to protect government installations, like military bases, or can be used abroad in an anti-aircraft artillery role in the field. The United States Marine Core 2nd Low Altitude Air Defense (LAAD) unit could be a potential user of the ISLAND system [10]. The team will consist of a gunner, a spotter, and a communications officer. The gunner will be responsible for carrying the launcher with additional missile munitions. The spotter will be responsible for additional missile munitions, targeting optics, as well as providing team security. The communications officer will carry communication systems to interface with command and control as well as additional missile munitions. The communications officer will relay intelligence to the team regarding potential UAVs threats and be responsible for communicating mission operating procedure and rules of engagement (ROE) against identified threats.

In its deployment, the ISLAND missile system will depend on communications with local command and control through defined operating areas to alert the team to threats, friendly assets, and non-combatants. Initial threat detection will likely occur from locally deployed radar assets, visually identified by combat units, or through local intelligence assets.

The ISLAND concept of operations (CONOPS) is shown in Figure 5. First, the potential threat is detected and identified. If it is determined that the threat can be engaged per the ROE, the user will launch the missile. The missile

will accelerate and track the target while gaining an advantageous position to initiate endgame maneuvers to destroy or disable the target. For one hour, the user will have to reload, detect the next target and launch the missile within six minutes, to successfully eliminate the UAV raid.
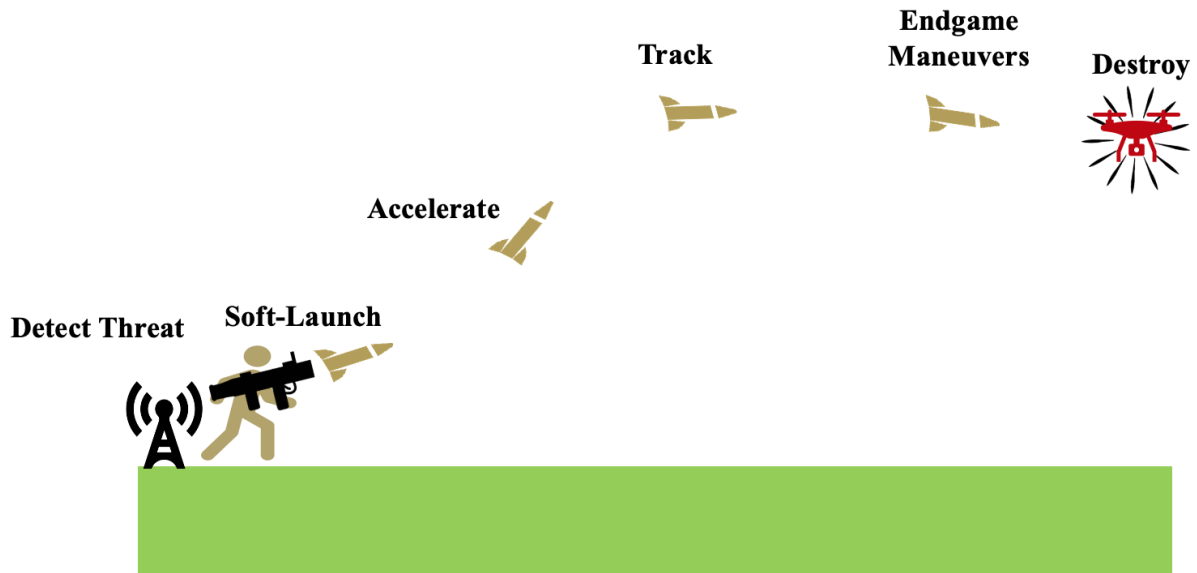
Figure 5: Concept of Operation for ISLAND

3   Configuration Analysis

With the requirements defined, a high level configuration analysis can begin. The configuration analysis is performed by dividing the missile into subsystems and investigating currently deployed systems. The configuration analysis used three weapons systems to develop alternatives for the launch system: the Raytheon Coyote Block 1 cUAS, which uses mechanical or compressed gas to launch, the Javelin, which uses an integrated launch and flight motor, and the Raytheon Stinger, which uses an ejectable rocket motor at launch [11][12]. The purpose of this exercise is to consider many different alternatives, no matter how unconventional, to keep the design space open. The initial Morph Matrix is shown in Figure 6.

ISLAND

Seeker	Infrared	Laser Designation	Semi-Active Radar	Active Radar	Image Recognition
Nose Design	High Fineness	Low Fineness	Ogive	Faceted	
Payload	Net	Kinetic	Impact Fuse	Proximity Fuse	
Control Style	Tail Only	Canard + Tail	Wing + Tail	Thrust Vectoring	
Control Surface	All Movable	Flaps			
Control Storage	None	Wrap-around	Switchblade	Folded	
Maneuvering	Skid-to-Turn	Bank-to-Turn	Rolling Airframe		
Motor Type	Solid	Liquid	Gas Turbine		
Launch System	Mechanical	Soft Launch	Ejectable Soft Launch	Compressed Gas	
Motor Casing	Steel Alloy	Titanium Alloy	Graphite/ Polyamide		
Missile Airframe	Aluminum Alloy	Steel Alloy	Titanium Alloy	Graphite/ Epoxy	Graphite/ Polyamide
Launch Tube	Aluminum Alloy	Composite/ Epoxy			

Figure 6: Initial Morphological Matrix

The initial Morph Matrix has 18.6 million combinations. It would be infeasible to conduct a study on every combination. Therefore, configuration down selection must occur to simplify the problem. Reasons for down selection are described below and the down selected Morphological Matrix is shown in Figure 7.

- Infrared and laser designation seekers are eliminated because they are ineffective against small targets and targets that do not emit a heat signature. Active radar is eliminated due to cost.

- The high fineness and faceted nose types are eliminated due to incompatibility with the seeker. The finesse and bluntness parameters can be explored using continuous variables.

- Net and kinetic payloads are eliminated due to ineffectiveness against Type 1 and 2 UAVs.

- Wing control is eliminated due to packaging concerns and the mission type, while thrust vectoring control is eliminated due to cost and over-complexity.

- Flap based control surfaces are eliminated due to cost and over-complexity.

- Folded control surfaces are selected due to simplicity.

- Bank-to-turn and rolling airframe maneuvers are eliminated due to over-complexity.

- Liquid and gas turbine propulsion systems are eliminated due to inability to meet 10 year storage without maintenance requirement.

ISLAND

- Mechanical launch is eliminated because of shoulder launched integration issues.

- Steel and Aluminum alloys are selected over exotic materials to minimize the cost.

						Down Selection Criteria
Seeker	Infrared	Laser Designation	Semi-Active Radar	Active Radar	Image Recognition	Ineffective against Type 1 & 2 UAV, high cost
Nose Design	High Fineness	Low Fineness	Ogive	Faceted		Seeker type incompatibility
Payload	Net	Kinetic	Impact Fuse	Proximity Fuse		Ineffective against Type 1 & 2 UAV
Control Style	Tail Only	Canard + Tail	Wing + Tail	Thrust Vectoring		Poor packaging, high cost and overcomplexity
Control Surface	All Movable	Flaps				High cost and overcomplexity
Control Storage	None	Wrap-around	Switchblade	Folded		Overcomplexity
Maneuvering	Skid-to-Turn	Bank-to-Turn	Rolling Airframe			Overcomplexity
Motor Type	Solid	Liquid	Gas Turbine			Maintenance requirements
Launch System	Mechanical	Soft Launch	Ejectable Soft Launch	Compressed Gas		Shoulder launch integration capabilities
Motor Casing	Steel Alloy	Titanium Alloy	Graphite/ Polyamide			Cost
Missile Airframe	Aluminum Alloy	Steel Alloy	Titanium Alloy	Graphite/ Epoxy	Graphite/ Polyamide	Cost
Launch Tube	Aluminum Alloy	Composite/ Epoxy				Cost

Figure 7: Down selected Morphological Matrix

Not every configuration could be eliminated, instead some subsystems required further trade studies and technical analysis. These subsystems are placed into a Trade-Study Morph Matrix, shown below in Figure 8. There are 24 combinations and the final down selections will be made using the design environment.

				Trade Study
Seeker	Image Recognition	Semi-active Radar		Vary sensor noise and payload type to trade missile accuracy and cost
Payload	Impact Fuse	Proximity Fuse		
Control Style	Tail Only	Canard + Tail		Vary aerodynamic configuration to trade missile mission range & maneuverability
Launch System	Soft Launch	Ejectable Soft Launch	Compressed Gas	Vary type of launch system to trade missile launch noise and acceleration

Figure 8: Trade-Study Morphological Matrix

4 Approach

There is a need to size the missile and to perform trade studies on the configurations outlined in the Trade-Study Morph Matrix above. To fulfill these needs, a missile design environment is developed. A Design Structure Matrix (DSM) for the environment is shown in Figure 9. Along the diagonal, in the gold, are the disciplines. In the upper triangle, there are blue boxes which represent outputs that are fed forward. In the bottom triangle, there are blue boxes which represent overall environment outputs or outputs that are fed backward.
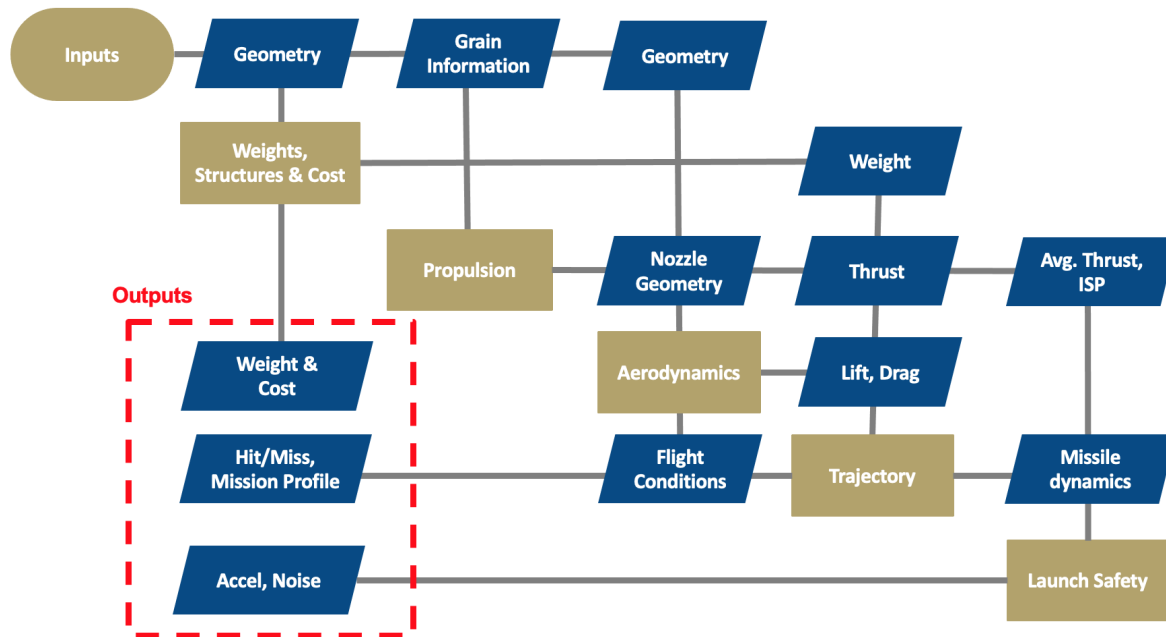
Figure 9: Design Structure Matrix

The following sections detail the technical approach and physics behind each discipline in the missile design environment.

4.1 Geometry

The missile architecture is split into a four groups: control surfaces, boattail, body, and nose. Each of these groups is assigned two or more continuous variables. The control surfaces parameters include the number of surfaces and several geometric parameters defining the airfoil sizing. The geometric parameters include root chord, taper ratio, aspect ratio, leading edge thickness angle, leading edge sweep angle, and location of max thickness.
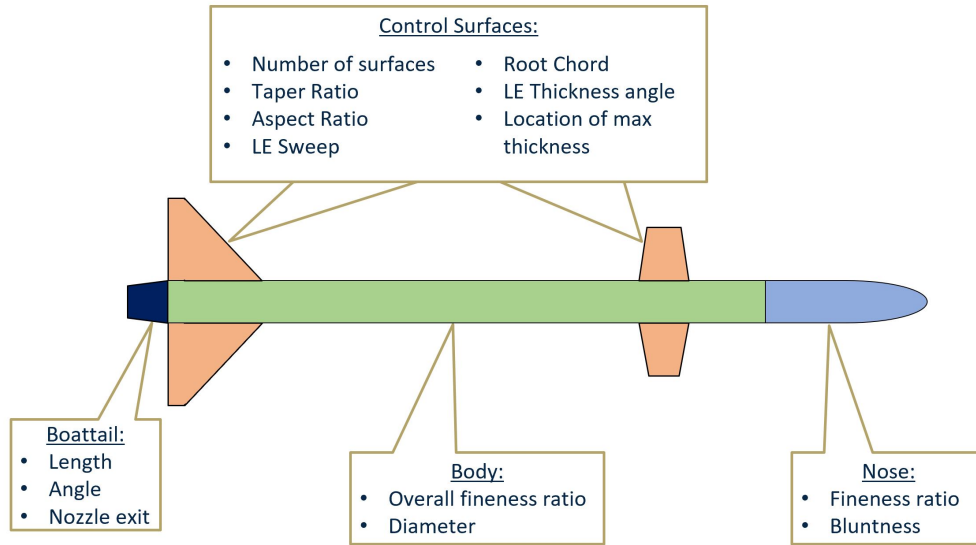
Figure 10: Geometry Variables

Many of the variables in the figure above are inputs into the overall environment. The body fineness ratio, nozzle diameter and body diameter are calculated using the results from the other disciplines.

4.2   Weights, Structures, and Cost

In this section, the methodology for calculating the missile weight, structural thickness and cost is outlined.

4.2.1   Weight Analysis

Launch weight is a critical factor that is input into the trajectory design environment. In the conceptual design stage, the launch weight is derived from published correlations. It is assumed that all subsystem weights account for their respective airframe structure. The volume of the guidance, navigation, and control (GNC) system is estimated based on a correlation relating design range, R, to GNC volume. Then, the mass is derived using the GNC volume [13]. The correlations are shown below in Equation (1) and (2).

$$V_{GNC} = 0.0038R^{1.38} \qquad (1)$$

$$m_{GNC} = 78V_{GNC}^{0.69} \qquad (2)$$

The GNC weight includes "all of the mechanical and electronic equipment necessary to guide the missile to the target." This includes the seeker and the control surface actuators as well as the body tube [13]. The correlation was

developed in the year 1986 and it is reasonable to assume that circuit board technology has advanced and electronics have become lighter. Thus, a 0.7 factor is applied to the calculated GNC weight.

The volume of the warhead is also determined from a published correlation relating mass of the warhead to the volume [13]. This mass value is a continuous variable and can be changed depending on miss distance performance. The correlation is shown below in Equation (3).

$$V_{warhead} = (m_{warhead}/109.5)^{(1/0.83)} \tag{3}$$

The propulsion weight is also determined from a series of empirical correlations to estimate the weight of the igniter, nozzle, and insulation [14]. The casing weight and the propellant weight are estimated using the definition of mass: density times volume. The equations for propulsion mass are shown in Equation (4) to (9).

$$m_{igniter} = 0.1502V_c^{0.571} \tag{4}$$

$$m_{nozzle} = 0.6066m_{propellant}^{0.6543} \tag{5}$$

$$m_{insulation} = 1.7*10^{-7}m_{propellant}^{-1.33} \cdot t_{burn}^{0.965}(L/D)^{0.144}A_{wall}^{2.69} \tag{6}$$

$$m_{propellant} = \rho_{propellant}V_{propellant} \tag{7}$$

$$m_{casing} = \rho_{casing}V_{casing} \tag{8}$$

$$m_{propulsion} = m_{igniter} + m_{nozzle} + m_{insulation} + m_{propellant} + m_{casing} \tag{9}$$

The control surface mass is estimated by calculating the volume, assuming a constant thickness surface. The mass is then found by definition. The relationships are shown in Equation (10) and (11).

$$m_{surfaces} = V_{surfaces}\rho_{surface} \tag{10}$$

$$V_{surfaces} = n_{surfaces}S_{surface}t_{surface} \tag{11}$$

Thus the mass of the entire missile is the sum of each subsystem, as shown in Equation (12).

$$m_{missile} = \sum m_{subsystems} = m_{propulsion} + m_{GNC} + m_{surfaces} + m_{warhead} \tag{12}$$

The length of the missile can be found using the volume of the subsystem, and the diameter of the missile, which is defined as the casing diameter plus twice the insulation thickness. This is shown below in Equation (13) and Equation

(14).

$$d_{missile} = d_{casing} + 2t_{insulation} \tag{13}$$

$$L_{missile} = \sum \frac{V_{subsystem}}{\pi(d_{missile}/2)^2} \tag{14}$$

4.2.2   Structural Analysis

To complete the structural analysis of the missile at this conceptual design phase, forces acting on the missile will be assumed as shown in the simplified free body diagram shown below in Figure 11.
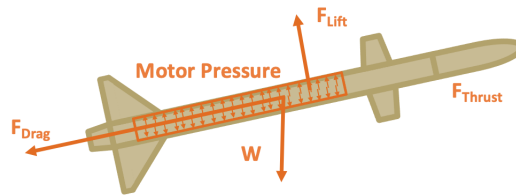
Figure 11: Free Body Diagram for Structural Analysis

The forces include axial forces of thrust and drag, aerodynamic lift forces from maneuvers, missile weight, and internal motor pressure. These values will be output from the final trajectory analysis for a given missile DoE case. From the forces acting on the missile, the structural thickness can be calculated for the motor casing and the structural airframe. In calculating the thickness, six load conditions are evaluated. First is a minimum gauge thickness for manufacturing as there is a minimum strength that will be required to resist the force of the tooling and fixtures. Next, buckling conditions will need to be evaluated from the bending moment due to maneuvers and the axial loading from thrust and drag. Following buckling, the thickness will need to be evaluated in yielding from the maneuver and axial loading. For this conceptual design phase, the values considered will be the maximum seen during the design mission profile. Finally, the thickness for the motor casing will be calculated using the peak internal motor pressure from the propulsion simulation. The thickness calculations are shown below in Equations 15 to 20.

$$t_{mfg} = 0.7d[[p_{ext}/E]l_{missile}/d]^{0.4} \tag{15}$$

$$t_{thrust} = T/2\pi\sigma r^2 \tag{16}$$

$$t_{buckling,bending} = 2.9r\sigma/E \tag{17}$$

$$t_{bending} = M/\pi\sigma r^2 \tag{18}$$

$$t_{buckling,compression} = 4.0r\sigma/E \tag{19}$$

$$t_{pressure} = p_{int}r/\sigma \tag{20}$$

After the thickness calculations are completed for each of the previous conditions, a root sum of squares (RSS) approach will be used with an appropriate factor of safety (FOS) to arrive at a material thickness value.

$$t_{overall} = FOS\sqrt{t_{mfg}^2 + t_{buckling,bending}^2 + t_{bucking,compression}^2 + t_{thrust}^2 + t_{bending}^2 + t_{pressure}^2} \tag{21}$$

4.2.3 Factor of Safety Calculation

The FOS used in the material thickness calculations will be based on published values such as those various military standards. Equation 21 is used for the calculating the thickness of the motor and airframe, and a FOS of 1.50 will be used on the applied loads and on the final thickness [15].

4.2.4 Material Selection

In an effort to reduce manufacturing costs, the airframe will be made from seamless drawn aluminum tubing with welded bulkheads made from machined billet aluminum. The nose cone and control surfaces will be machined from solid billet aluminum. If the production scale and strength margins exist, the use of aluminum castings for the nose cone and internal bulkheads can be considered. For the motor casing, alloy steel was qualitatively determined to be the best option, given the cost constraints and the motor's operating conditions. 4130 alloy steel will be used in the motor casing with the main body machined from seamless drawn tubing. The casing will be welded to the forward dome and aft nozzle sections, both machined from billet 4130 steel alloy. 4130 steel alloy is used for its acceptable strength attributes at the high motor operating temperature and its resistance to buckling during flight loads. 4130 steel also has superior qualities for machining and welding which will reduce cost and development time associated with the development of the missile for production. Material properties are detailed in Table 5.

Table 5: Material Proprieties for Structural Analysis

Material	Density (lb/in^3)	Yield Strength (psi)	Ultimate Strength (psi)	Modulus of Elasticity (ksi)
Aluminum 2219	0.103	42,100	58,000	10,600
Steel 4130	0.2819	63,100	97,200	29,700

4.2.5 Cost and Manufacturing

Cost estimates for the ISLAND system are estimated from correlations published in Fleeman, which are then adjusted with additional factors based on manufacturing difficulty and technology maturity. Two cost numbers are derived from the correlations, the first being cost for the system design and development (SDD). This correlation is based on the time duration of 21 previous missile development programs and is show in Equation (22) [15].

$$C_{SDD} = 20(10^6)t_{SDD}^{1.9} \tag{22}$$

Where t_{SDD} is the program time in years and the result is in 1999 USD. Following the cost estimate for the design and development, a correlation is used to determine the individual missile unit cost for the ISLAND program. This correlation is based on a regression to the unit production cost of the 1000th missile from current and historical programs based on the launch weight of the missile. This regression is shown in Equation (23) [15].

$$C_{1000} = 6100W_L^{0.758} \tag{23}$$

A summary of the discipline inputs, outputs, and assumptions are shown in Table 6.

Table 6: Table of Inputs, Outputs and Assumptions for Weight, Structures and Cost Module

Inputs	Outputs	Assumptions
Range	Missile Mass	0.7 Factor on GNC Weight
Warhead Mass	Missile Length	1.50 Ultimate Factor of Safety
Missile Diameter	Unit Cost	1.15 Yielding Factor of Safety
Propulsion Mass	Development Cost	
	Structure Thickness	

It is decided that the structural thickness is not an important metric during sizing and trade studies. Thus, the structures will be evaluated only for the final design.

4.3 Propulsion

The propulsion system had to be designed to meet multiple requirements, including the launch acceleration, launch noise, weight, and user safety requirements. In the configuration analysis above, a solid rocket motor was selected as the primary propulsion system type and its design process will be discussed in the upcoming sections.

4.3.1   Solid Rocket Motors

Solid rocket motors are commonly used in air-to-ground, ground-to-air, and booster rockets, due to their simplicity and stability in long term storage. To model the solid rocket motor (SRM) for ISLAND, an internal ASDL tool called Solid Motor Development Code (SMAC), was used [16]. SMAC's current capabilities allow users to vary multiple design, geometry, and propellant variables to output SRM specifications such as: thrust and pressure curves, motor dimensions, and system weight. These outputs provide the necessary information for trajectory to conduct its mission and to determine whether the safety requirements are met.

SMAC works by first defining the SRM geometry and then feeding the results into a geometric burn simulation. The geometry module uses an edge finding algorithm to converge on a nozzle geometry as well as a propellant geometry. The burn simulator models the motor burn via a unsteady lumped parameter burn algorithm [16]. An example of the burn simulation is shown in Figure 12.
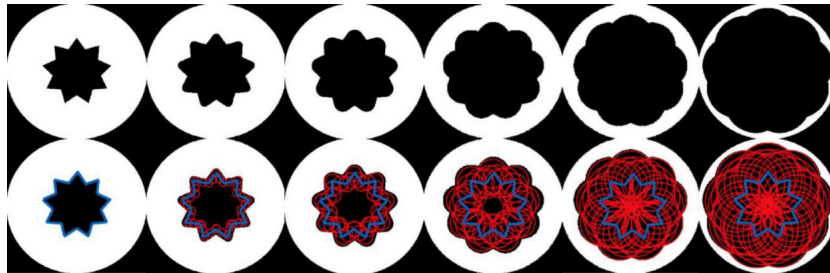
Figure 12: Example of a SMAC's burn simulation [16]

In order to evaluate some of the alternatives in the Trade Study Morph Matrix, SMAC is modified to solve for the characteristics of a two stage motor, that shares a common nozzle for both stages.

For solid rocket motors, the grain geometry is the driving factor for motor cost and performance. BATES grains, or tubular grains, have progressive burn times, where star grains have more steady burn times, and multi-fin grains have large thrust profiles very early in the burn, but quickly reduce to low thrust for the remainder of the burn. The difference between the grain geometries is shown in Figure 13.
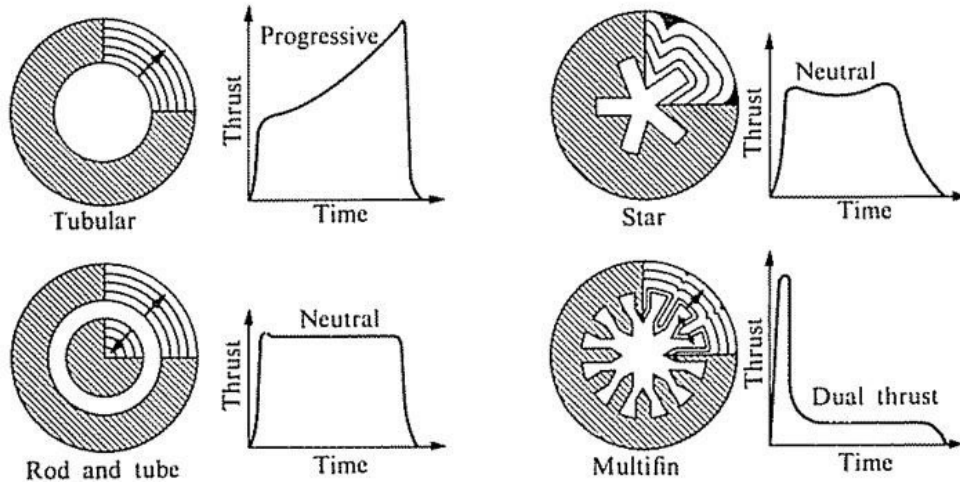
Figure 13: Solid Rocket Motor Grains and their Thrust Profiles [17]

Due to the short design range, low launch acceleration and low noise requirement, a BATES grain was selected for further analysis, with possible implementation of an end-burn geometry to boost the missile speed and increase maneuverability in the endgame. A BATES grain is also the cheapest and simplest to manufacture, reducing the unit cost.

A standard commercially available Ammonium Perchlorate Composite Propellant (APCP) is selected for the preliminary design. Its characteristics were experimentally determined by the Georgia Tech Experimental Rocketry Club and the results are shown in Table 7.

Table 7: Propellant Characteristics used in ISLAND Preliminary Design

Burn Rate Coefficient (psi)	Pressure Exponent (psi)	Propellant Density (slug/in^3)	Characteristic Velocity
0.027	0.3	0.00176	4890

A summary of the discipline inputs, outputs, and assumptions are shown in Table 8.

Table 8: Table of Inputs, Outputs and Assumptions for Propulsion Module

Inputs	Outputs	Assumptions
MEOP	Thrust Curve	Grain Type: BATES
Grain Diameter	M-dot Curve	Propellant Type: APCP with characteristics in Table 7
Grain Inner Diameter	Nozzle Geometry	Density of Motor Casing: 0.284 lb/in^3 (4130 Steel)
Grain Fineness Ratio	Insulation Geometry	Density of Insulation: 0.0311 lb/in^3 (EPDM Rubber)
	Casing Geometry	
	Subsystem Mass	

4.4 Aerodynamics

The purpose of the aerodynamics discipline is to link missile geometry and flight conditions to the aerodynamic forces produced by the missile. This discipline environment needed to be capable of producing lift and drag forces for each time step when interfaced with the trajectory code. In addition, the aerodynamics code needed to be able to size and verify stability and maneuverability requirements for individual on-design and off-design scenarios. The chosen methodology that fits these calculation requirements is the conceptual design aerodynamics approach described in Fleeman's Tactical Missile Design book [15]. The aerodynamic predictions generated with this code are based on flight conditions, geometry, historical regressions, and other derivations as described in Fleeman. The process walks through the build up of axial and normal force coefficient calculations for the nose, body, boat tail, and any additional surfaces. One assumption made during this build up process is that the aerodynamic axial force coefficient is dominated by the zero-lift drag coefficient, so we assume that these are equal, as shown in Equation (24). A notional build up of the normal force coefficient is shown in Equation (25). After these force coefficients are determined, basic transformations can be applied to adjust axial and normal into lift and drag, as shown in Equations (26) and (27) respectively. The following sub-sections will breakdown the individual missile contributions for Equations (24) and (25).

$$C_A = C_{D0} = (C_{D0})_{Body} + (C_{D0})_{Canard} + (C_{D0})_{Tail} \tag{24}$$

$$C_N = (C_N)_{Body} + (C_N)_{Canard} + (C_N)_{Tail} \tag{25}$$

$$C_L = C_N cos\alpha - C_{D0} sin\alpha \tag{26}$$

$$C_D = C_N sin\alpha - C_{D0} cos\alpha \tag{27}$$

4.4.1 Missile Body

The drag forces on the missile body are further broken down into the friction drag induced on the missile skin, the wake drag produced by the missile base, and the wave drag at the missile nose during supersonic flight. The friction drag is directly related to the length of the missile and the flight conditions. The wake drag is highly dependent on whether or not the motor is firing. If the motor is firing then there is less aft area to create a wake. To further reduce this aft area, a boat tail is often added. The wave drag is coupled with the nose fineness, so if the mission takes place in the supersonic regime, then the drag could be reduced with a longer nose length. Equations (28) through (33) show in detail the equations used to calculate the drag on the body.

$$(C_{D0})_{Body} = (C_{D0})_{Body,Friction} + (C_{D0})_{Base} + (C_{D0})_{Body,Wave} \tag{28}$$

$$(C_{D0})_{Body,Friction} = 0.053(l/d)[M/(ql)]^{0.2} \tag{29}$$

$$(C_{D0})_{Base,Coast} = \begin{array}{ll} 0.25/M & M > 1 \\ 0.12 + 0.13M^2 & M < 1 \end{array} \tag{30}$$

$$(C_{D0})_{Base,Powered} = \begin{array}{ll} (1 - A_e/S_{Ref})(0.25/M) & M > 1 \\ (1 - A_e/S_{Ref})(0.12 + 0.13M^2) & M < 1 \end{array} \tag{31}$$

$$(C_{D0})_{Body,Wave} = \begin{array}{ll} 3.6/[(l_N/d)(M-1)+3] & M > 1 \\ 0 & M < 1 \end{array} \tag{32}$$

$$(C_{D0})_{Wave,Blunt} = (C_{D0})_{Wave,Sharp}(S_{Ref} - S_{Hemi})/S_{Ref} + (C_{D0})_{Wave,Hemi}\frac{S_{Hemi}}{S_{Ref}} \tag{33}$$

The normal force produced by the missile body is dependent upon the body shape and the angle of attack. The missile could have a lifting body, elliptical cross section, or a non-lifting body, circular cross section. Based on the Morph Matrix, a circular cross section is selected, thus $\Phi = 0$ since it is not needed to define an incidence angle of a circle. The equation to predict the normal force coefficient of the body is shown in Equation (34).

$$|C_N| = |(a/b)cos\Phi + (b/a)sin\Phi|(|sin(2\alpha)cos(\alpha/2)| + 2(l/d)sin^2\alpha) \tag{34}$$

Equation (35) shows the equation to find the center-of-pressure location for the body as a function of angle of attack and the length ratio between the body and the nose. This will be used with stability.

$$(x_{AC})_B/l_N = 0.63(1 - sin^2\alpha) + 0.5(l_B/l_N)sin^2\alpha \tag{35}$$

Equation (36) shows the equation to find the normal force curve slope due to angle of attack for the missile body. This will also be used with stability.

$$(C_{N\alpha})_{Body} = 2(\frac{a}{b}cos(\Phi) + \frac{b}{a}sin(\Phi)) \tag{36}$$

19

4.4.2 Missile Control Surfaces

The drag forces on the missile control surfaces are further broken down into the friction and wave drag similar to the body. It was assumed that the deflection of the control surfaces was zero throughout our sizing process and instead the entire missile pitches to meet force requirements. This assumption was made because the trajectory code would have needed to include a more advanced control system to leverage the surface deflection. The equations used to compute the drag for the missile surfaces are shown in Equations (37) through (39).

$$(C_{D0})_{W,Friction} = n_W[0.0133/(qc_{mac})^{0.2}](2S_W/S_{Ref}) \tag{37}$$

$$(C_{D0})_{W,Wave} = [\frac{2n_W}{(\gamma M_{LE}^2)}]\{\{\{\frac{[(\gamma+1)M_{\Lambda LE}]}{2}\}^{\frac{\gamma}{\gamma-1}}\{\frac{(\gamma+1)}{[2\gamma M_{\Lambda LE}^2 - (\gamma-1)]}\}^{\frac{1}{\gamma-1}} - 1\}sin^2\delta_{LE}cos\Lambda_{LE}\frac{t_{mac}b}{S_{Ref}} \quad M_{\Lambda LE} = Mcos\Lambda_{LE} > 1 \tag{38}$$

$$(C_{D0})_{Wing} = (C_{D0})_{W,Wave} + (C_{D0})_{W,Friction} \tag{39}$$

Next, the normal force coefficients for any surfaces on the missile need to be calculated. Linear wing theory and Newtonian impact theory are applied to low aspect ratio surfaces $AR \leq 3$. These relationships are summarized in Equation (40), where $\alpha' = \alpha + \delta$, where δ is the canard deflection. For preliminary design, δ is always assumed to be 0.

$$|(C_N)_{Wing}| = [4|sin\alpha'cos\alpha'|/(M^2-1)^{1/2} + 2sin^2\alpha']\frac{S_W}{S_{Ref}} \quad M > \{1 + [\frac{8}{(\pi AR)}]^2\}^{1/2}$$

$$|(C_N)_{Wing}| = [(\pi AR/2)|sin\alpha'cos\alpha'| + 2sin^2\alpha']\frac{S_W}{S_{Ref}} \quad M < \{1 + [\frac{8}{(\pi AR)}]^2\}^{1/2} \tag{40}$$

Equation (41) shows the equation to find the center-of-pressure location for a surface as a function of Mach number and aspect ratio. This will be used with stability.

$$(\frac{x_{AC}}{c_{MAC}})_{Wing} = \begin{matrix} \frac{[AR(M^2-1)^{1/2}-0.67]}{[2AR(M^2-1)^{1/2}-1]} & M > 2 \\ 0.25 & M \approx 0 \end{matrix} \tag{41}$$

Equation (42) shows the equation to find the normal force curve slope due to angle of attack for the missile control surfaces. This will also be used with stability.

$$(C_{N\alpha})_{Wing} = \begin{matrix} \frac{4}{\sqrt{M^2-1}} & M^2 > 1 + (\frac{8}{\pi AR})^2 \\ \pi\frac{AR}{2} & M^2 < 1 + (\frac{8}{\pi AR})^2 \end{matrix} \tag{42}$$

4.4.3 Missile Stability

To calculate stability requirements, Equation (43) was rearranged to instead solve for the canard center of pressure location. This leaves canard chord and tail chord as free variables. The tail location is fixed to the base of the body tube for all configurations.

$$\frac{(S_T)_{Req}}{S_{Ref}} = \left\{ (C_N\alpha)_B \frac{[x_{CG} - (x_{CP})_B]}{d} + (C_N\alpha)_W \left\{ \frac{[x_{CG} - (x_{CP})_W]}{d} \right\} \right\} / \left\{ \left\{ \frac{[(x_{CP})_T - x_{CG}]}{d} \frac{S_W}{S_{Ref}} \right\} (C_N\alpha)_T \right\} \quad (43)$$

The implementation of the aerodynamics environment was verified against an air-to-air example sizing case in Fleeman [15]. The results of the verification are shown in Table 9. The majority of this error is due to the truncation and rounding of arithmetic presented in the text.

Table 9: Aerodynamics Environment Verification Results

Value	Fleeman	Aerodynamics Environment	% Error
Missile Normal Force Coefficient	11.1	11.048	0.47%
Missile Drag Coefficient	1.06	1.053	0.66%

A summary of the discipline inputs, outputs, and assumptions are shown in Table 10. Fleeman's estimate for wave drag produced by a surface is based on a double wedge airfoil defined by a leading edge thickness angle and location of maximum thickness. From initial trajectory analysis, it was assumed that the missile would spend time in the transonic regime and thus double wedge airfoils are applicable to the mission and the provided equations can be used. It was assumed that the maximum thickness would be located at the quarter chord and the leading edge thickness angle would be driven by a maximum thickness constraint.

Table 10: Table of Inputs, Outputs and Assumptions for Aerodynamics Module

Inputs	Outputs	Assumptions
Surface Geometry	Lift	Airfoil Type: Double Wedge
Body Geometry	Drag	Location of Max Thickness: 0.25c
Boat-tail Geometry	Max Maneuverability	4 Surfaces per Tail/Canard
Nose Geometry	Stability Information	
	2D sketch	

4.5 Trajectory

The purpose of the trajectory discipline is to carry the missile through its design mission and to determine whether or not the missile hits the target and meets additional requirements. To carry out its goal, the trajectory environment

ISLAND

uses results from the weight, aerodynamics, and propulsion environments. The following subsections will outline the equations of motion, trajectory propagation, trajectory guidance, and the sensor modeling.

4.5.1 Equations of Motion

The equations of motion for the missile and the target model the kinematics of the system. A three degree of freedom (3-DOF) system was implemented because the requirements only specify a downrange objective. A 3-DOF system is preferred over a full 6-DOF system because of the reduction in run time and complexity. Furthermore, control design is not the goal of the preliminary trajectory environment so a 6-DOF system is not needed. A flat earth assumption is made because the objective range is small, only 3.5 nautical miles.

Because a 3-DOF system is chosen, only movement in the horizontal, vertical and pitch directions is modeled. The state of the system is shown below in Equation (44).

$$
\begin{bmatrix} \dot{x} \\ \dot{y} \\ \dot{v}_x \\ \dot{v}_y \\ \dot{\alpha} \\ \dot{m} \end{bmatrix} = \begin{bmatrix} v_x \\ v_y \\ F_x/m \\ F_y/m \\ q \\ \dot{m} \end{bmatrix}
\tag{44}
$$

The missile experiences lift and drag forces that are parallel and perpendicular, respectively, to the wind direction. Thrust is always applied parallel to the roll axis since thrust vectoring is not used. A free body diagram is developed for the missile and it is shown in Figure 14.
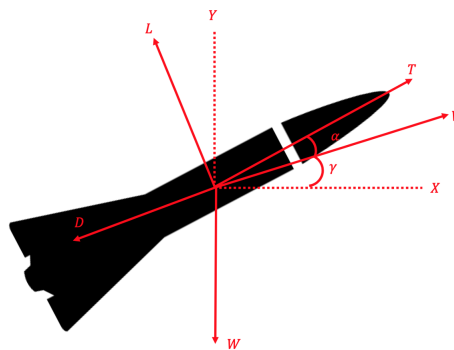
Figure 14: Free Body Diagram of the 3DOF Missile System

Using this diagram, the equations for the X and Y direction forces are derived. Equations (45) through (47) show equations for the X and Y direction forces as well important aerodynamic variables like flight path angle and pitch angle.

$$F_x = T\cos(\theta) - D\cos(\gamma) - L\sin(\gamma) \tag{45}$$

$$F_y = T\sin(\theta) - D\sin(\gamma) + L\cos(\gamma) - W \tag{46}$$

$$\gamma = \frac{v_y}{\sqrt{v_x{}^2 + v_y{}^2}} \tag{47}$$

$$\theta = \gamma + \alpha \tag{48}$$

The thrust and mass flow are found by interpolating the thrust and mass flow curves output by the propulsion environment. Aerodynamic forces were found by calling the aerodynamics module for each time step. Information such as angle of attack, Mach number, dynamic pressure, and whether or not the missile was powered was input into the module. The following equations were used to model the standard atmosphere:

$$T = T_0 + ah \tag{49}$$

$$P = P_0 \left(\frac{T}{T_0}\right)^{\left(\frac{-g_0}{aR}\right)} \tag{50}$$

$$\rho = \rho_0 \left(\frac{T}{T_0}\right)^{\left(\frac{-g_0 + aR}{aR}\right)} \tag{51}$$

In the equations above, a represents the slope of temperature with respect to altitude, h represents altitude, R represents the ideal gas constant, g_0 represents the sea level gravitational acceleration and T_0, P_0 and ρ_0 represent the sea level standard temperature, pressure and density.

For preliminary sizing, the target is modeled as a hovering target at 3.5 nautical miles, 5,000 ft. Capability does exist to test a moving and accelerating target during detailed design.

4.5.2   Trajectory Propagation

The purpose of trajectory propagation is to move the missile or target state one time step. The environment implements the fourth order Runge Kutta method (RK4) to propagate the target and missile [18]. Because the equations of motion

are of the form $\dot{x} = f(x_i, t_i)$, Equations (52) through (56) can be used to solve for the state in the next time step.

$$k_1 = f(x_i, t_i) \tag{52}$$

$$k_2 = f(x_i + k_1 \frac{h}{2}, t_i + \frac{h}{2}) \tag{53}$$

$$k_3 = f(x_i + k_2 \frac{h}{2}, t_i + \frac{h}{2}) \tag{54}$$

$$k_4 = f(x_i + k_3, t_i + h) \tag{55}$$

$$x_{i+1} = x_i + \frac{h}{6}(k_1 + 2k_2 + 2k_3 + k_4) \tag{56}$$

The time step, h, is held constant at 0.1 seconds for a majority of the flight. When the missile travels within 300 ft of the target, the time step decreases to 0.01 seconds. This selection of time steps provides good run time performance while not compromising endgame fidelity.

4.5.3   Trajectory Guidance

The purpose of the trajectory guidance is to control the vehicle by changing the pitch rate, q. For preliminary design, the pitch rate is assumed to have no lag. The sizing mission is either the objective mission or the threshold mission, as outlined in the requirements.

The guidance is broken down into three phases, launch, boost and tracking, each with its own control logic. The control logic uses noise measurements from the GPS/INS and the seeker. These measurements must be filtered using a Kalman filter before being used in the control algorithm.

Launch Phase

The launch phase lasts only 0.5 seconds, enough time for the missile to travel approximately 100 feet. The purpose of this phase is to gain speed as well as to travel directly away from the soldier, to minimize the noise when the flight motor ignites. During this phase, the missile guidance attempts to target a flight path angle, γ_0 of 45 degrees. This flight path angle will ensure a positive rate of climb during the launch phase and is similar to that of the Stinger missile [12].

A simple proportional controller is sufficient to achieve this task. Equation (57) shows the algorithm. In the equation below, the proportional gain, K_p, was set to 0.1.

$$q = K_{p,launch}(\gamma_0 - \gamma) \tag{57}$$

If a lower launch angle is chosen, $K_{p,launch}$ must be increased to ensure the missile does not have a negative climb rate.

Boost Phase   The purpose of the boost phase is to allow the missile to climb and gain speed. The inputs to this phase are the flight path angle and the time of the boost phase. These inputs are optimized using Python's Scipy Optimize package. The angle and time are optimized for each missile design and configuration. For better performance, the boost time is limited to 5 seconds maximum, and the angle is limited to 70 degrees. The missile guidance algorithm attempts to target the optimized flight path angle, γ_{opt}. As above, a simple controller is sufficient to achieve this task. Equation (58) shows the algorithm. In the equation below, the proportional gain, $K_{p,boost}$, was set to 0.1.

$$q = K_{p,boost}(\gamma_{opt} - \gamma) \tag{58}$$

Tracking Phase

The tracking phase lasts for the rest of the flight. The purpose of this phase is to track and hit the target. During this phase, the missile implements a proportional navigation algorithm, shown in Figure 15.
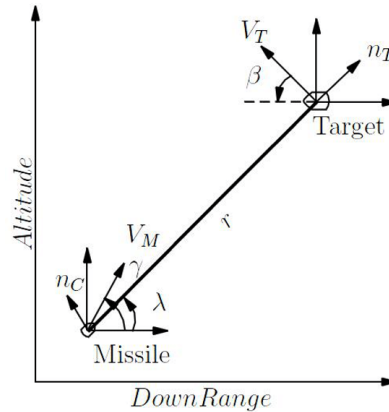
Figure 15: Diagram of proportional navigation [19]

The goal of proportional navigation is to maintain a constant line of sight (LOS) angle rate, $\dot{\lambda}_0 = 0$, between the target and the missile [19]. This is achieved by first using the GPS/INS and seeker filtered measurements to calculate the line of sight angle rate. A proportional integral derivative (PID) controller is used to drive this LOS angle rate to zero. Equations (59) through (61) show this calculation and the control algorithm. The gains are determined on a trail basis and are as follows $K_{p,track} = 5, K_{i,track} = 0.1$ and $K_{d,track} = 14$.

$$\lambda = atan(\frac{y_t - y_m}{x_t - x_m}) \tag{59}$$

$$e(t) = \frac{d\lambda}{dt} - \dot{\lambda}_0 \tag{60}$$

$$q = K_{p,track}e(t) + K_{i,track}\int e(t)dt + K_{d,track}\frac{de(t)}{dt} \tag{61}$$

A simple proportional (P) controller is insufficient to hit the target and results in very high oscillations. A proportional-derivative (PD) controller is sufficient to hit the target but has somewhat poor accuracy. The algorithm could be improved if a full PID controller is implemented. Care should be taken to ensure that integral gain is not too high otherwise the trajectory will flatten out. Figure 16 shows examples of the trajectory when different control algorithms are implemented.

$$K_p = 5, K_i = 0, K_d = 0$$

$$K_p = 5, K_i = 0, K_d = 14$$

$$K_p = 5, K_i = 1, K_d = 14$$

$$K_p = 5, K_i = 0.1, K_d = 14$$
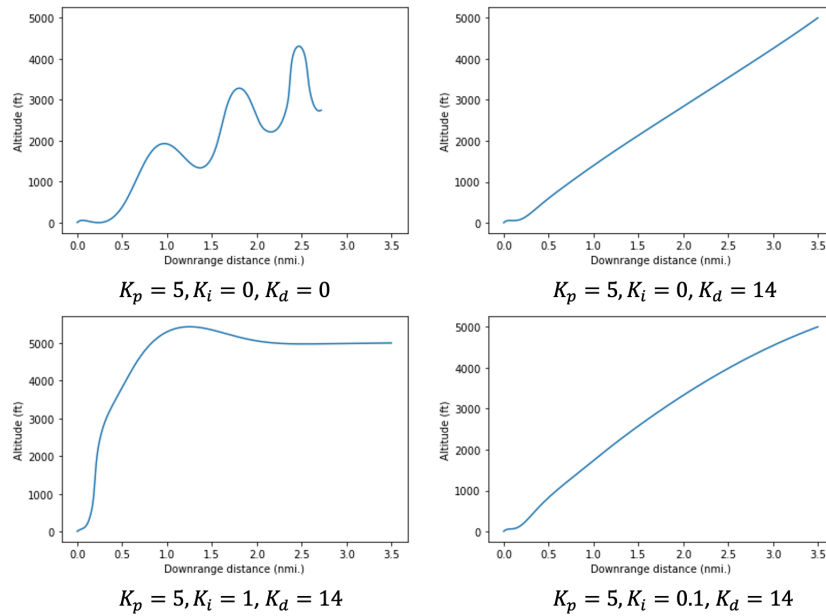
Figure 16: Comparison of different controller gains

The pitch rate, q, is limited by the maximum possible acceleration that can be generated from the aerodynamic surfaces. If the pitch rate exceeds the maximum allowable pitch rate it is updated as shown in Equation (62).

$$q = a_{max}/v \tag{62}$$

The different phases of the trajectory guidance, for a notional mission, are illustrated below in Figure 17.
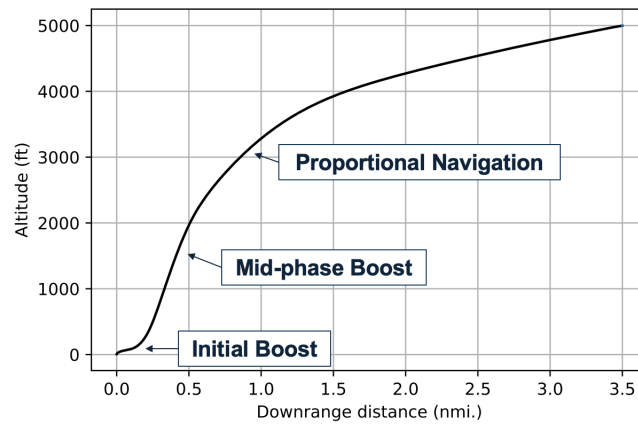
Figure 17: Phases of Guidance for a Notional Mission

4.5.4 Sensor Modeling and Kalman Filtering

The on-board sensors, which include the seeker and the GPS/INS system measure the missile position and velocity and the target position and velocity. Random noise is added to the actual values to simulate a more realistic sensor. To filter this noise, a simple Kalman filter was implemented.

The GPS/INS noise is modeled based off of a Rockwell Collins NAVSTRIKE GPS Reciever, which is commonly used on missile systems [20]. This state of the art sensor is ideally suited for ISLANDs purpose and offers low sensor noise and high update rate. The seeker noise is different based on the seeker type. Two options are evaluated, a Ku-Band semi active radar, similar to that used on the Raytheon Coyote, and an autonomous image recognition option. Table 11 summarizes the noise information for the GPS/INS and the seeker options.

Table 11: Noise characteristics for different sensors

Parameter	Rockwell Collins NavStrike GPS/INS [20]	Ku Band Seeker [21]	Image Recognition Seeker [22]
Position Standard Deviation (ft)	9.84	9.84	18.25
Velocity Standard Deviation (ft/s)	0.23	0.23	0.427*
Update Rate (Hz)	50	20	100

*assumed

Since there was little public information on image recognition seekers, the velocity standard deviation needed to be assumed. The image recognition seeker showed 1.85 times worse position standard deviation performance, compared

to the Ku-Band Seeker [22]. Therefore, the same factor was applied to the velocity standard deviation.

The measurement noise is modeled as independent randomly distributed Gaussian noise with 0 mean and standard deviation based on manufacturer specifications. Equation (63) shows the result.

$$\vec{x}_{measured} = \vec{x}_{real} + \mathcal{N}(0, \sigma^2) \tag{63}$$

The Kalman filter process can be broken down into two steps. A prediction step and a update step. The prediction step takes in the previous filtered state, x_{k-1}, to make a prediction of the filtered state, x_k, using the state transition matrix, A. In this step, the covariance, P_k is also estimated using the previous covariance, P_{k-1} , the state transition matrix from above and the process noise matrix, Q . In the update step, the Kalman gain is estimated based on the covariance, the measurement matrix H, and the measurement noise matrix, R. Finally, the filtered state and the covariance matrix are updated. The equations for the prediction step and the update step are shown below in Equations (64) to (68).

$$x_k = Ax_{k-1} \tag{64}$$

$$P_k = AP_{k-1}A^T + Q \tag{65}$$

$$K_k = P_k H^T (HP_k H^T + R)^{-1} \tag{66}$$

$$\vec{x}_{filtered,k} = \vec{x}_{filtered,k} + K_k(\vec{x}_{measured,k} - H\vec{x}_{filtered,k}) \tag{67}$$

$$P_k = (I - K_k H)P_k \tag{68}$$

The state transition matrix, A is found by solving dynamics of the system while the measurement matrix H is simply an identity matrix. The process noise matrix, is set to an arbitrarily low value by assuming disturbances and changes to the system are small. Finally, the measurement noise matrix, R, is a diagonal matrix with entries equal to σ^2. The process is the same regardless of if it is the GPS/INS sensor or the seeker sensor.

A summary of the discipline I/O and assumptions are shown in Table 12.

Table 12: Table of Inputs, Outputs and Assumptions for Trajectory Module

Inputs	Outputs	Assumptions
Aerodynamics	Mission Dynamics	Initial Missile State
Engine Deck	Miss Distance	Initial Target State
Weight		Kalman Filter Gains
		Guidance Controller Gains
		Standard Atmosphere
		Flat Earth

4.6   Launch Safety

The final discipline is the safety environment. This section will dive into the specifics of the launch noise and launch acceleration requirements, as well as outline how each metric was calculated.

4.6.1   Noise

Noise is a difficult parameter to simulate without real-life measurements of the noise across multiple frequencies at at least 2 locations. With measurement devices, experimental noise data is measured across an octave band frequency before weighting is applied across that octave band to calculate the total noise level using the sum of logarithmic power [23]. Per the RFP, the noise level within 100ft of the launch location shall be less than 120 dB(A). Different types of noise are produced by different mediums, and therefore classified differently depending on what kind of exposure is expected. Continuous noise, measured in dB(A), is classified as noise that remains constant and stable over time. Examples of this type of noise include noise from a construction site, airplane noise, noise from a busy highway, and music. For noise measured in dB(A), the threshold for pain is 85dB(A) [24]. Noise produced from gunfire, explosions, and missiles are classified as impulse noise, measured in dB(P) . For these types of noise sources, the noise is generated with short bursts or impulses, and typically only lasts for less than 100 to 200 ms. It is due to this short duration of noise that impulse noises are measured in dB(P), or with peak sound pressure levels. Where continuous noise is A-weighted, impulse noise is not weighted, and is a "raw" measurement of the sound pressure levels being produced [23]. The threshold for pain as per OSHA standards is 140 dB(P) [24]. Current military systems such a mortar launcher and MAAWS, multi-role, anti-armor, anti-personnel weapons systems fall within impulse noise ranges of 160 and 190 dB(P), as seen in Figure 18 [24]. Please note that the continuous noise scale and impulse noise scale are not correlated or comparable.
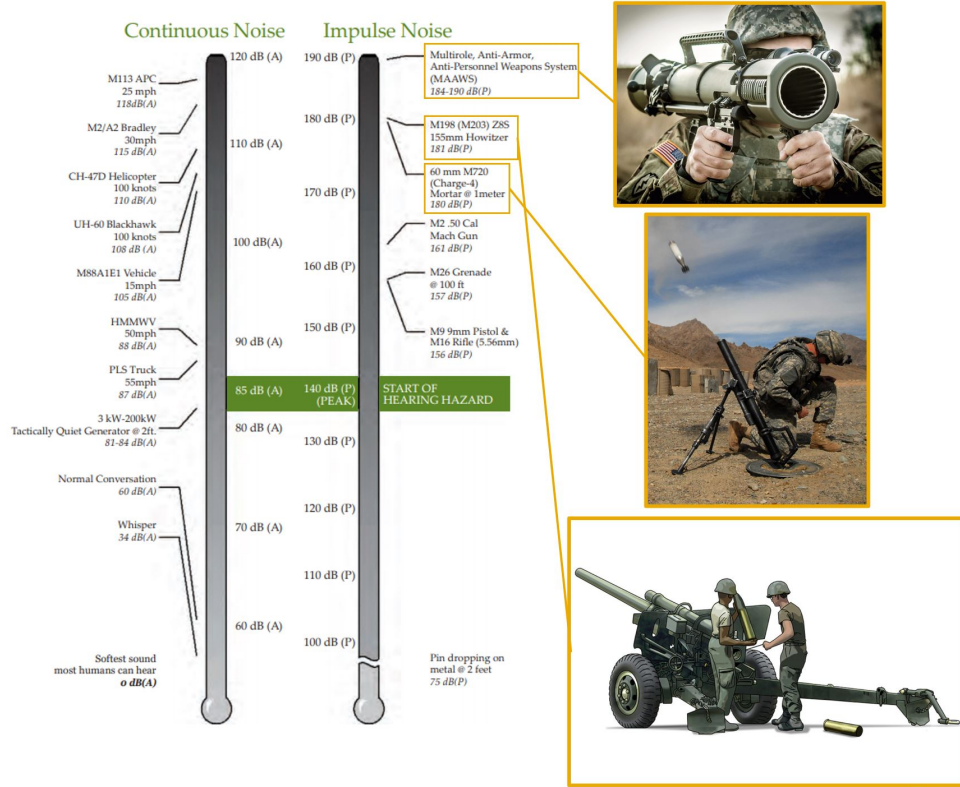
Figure 18: Noise Examples [24]

As a rule of thumb, sound output power will be between 0.5 to 1% of the mechanical power output of the engine. Ignoring directivity and the frequency dependence of atmospheric absorption with noise output being 1% of the mechanical power, sound pressure levels can be calculated with Equation (69), where T is thrust in pounds, I_{sp} is the specific impulse in seconds, and R is the distance from the source in feet [25].

$$SoundPressure\,(dBP) = 10log\,(T) + 10log\,(I_{sp}) - 20log\,(R) + 123dB \tag{69}$$

There is not, however, any direct conversion from dB(P) to dB(A), and vice versa. To convert unweighted noise levels in dB to A-weighted, a logarithmic sum of powers must be applied across the octave band frequencies with A-weighting factors applied at each octave band to determine the overall noise level in dB(A). To roughly estimate this weighting, a "worst case" scenario will be applied to the previously calculated sound pressure level to estimate what the equivalent dB(A) would be. The "worst case" weighting occurs at approximately 2500 Hz, as seen in Fig. 19. At 2500 Hz, approximately 1.5 dB is added to the measured sound level.
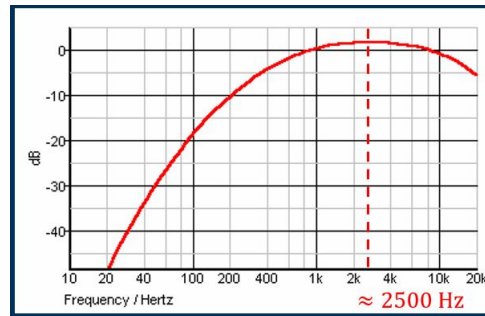
Figure 19: "Worst Case" dB(A) Weighting

The launch noise requirement brought forward by the RFP is strict, and therefore will be analyzed through 3 lenses:

1. Does the launch noise meet the RFP Requirement of 120dBA?

2. Does the launch noise fall within historical ranges of current existing systems?

3. Does the launch noise fall below standard noise thresholds?

The noise profile of the final design will be viewed as having met the noise safety requirement should it successfully answer any of the questions above.

4.6.2 Acceleration

To estimate the launch acceleration, a few assumptions are made. It is assumed that the only forces on the missile at launch are the missile weight and the thrust; aerodynamic forces and friction are deemed negligible. A launch angle of 45 degrees is assumed for the ISLAND missile. This launch angle is similar to that of the Stinger missile. With this information, and by drawing a simple free body diagram, the net forces on the missile in the tube direction, and thus the launch acceleration can be derived. The free body diagram is shown in Figure 20.
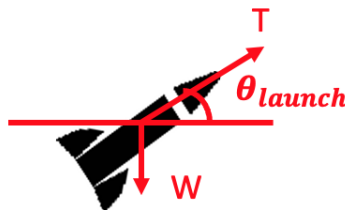
Figure 20: Launch Free Body Diagram

In this analysis, the normal force is ignored and only the forces that would accelerate the missile are considered.

This results in Equation (70).

$$F_{net} = m_{missile}a_{launch} = T_{launch} - W\sin(\theta_{launch})$$ (70)

This equation can be solved for a_{launch}, if the T_{launch} is known. As a initial estimate, the thrust over the first 0.5 seconds of the motor burn is averaged to find T_{launch}.

A summary of the discipline I/O and assumptions are shown in Table 12.

Table 13: Table of Inputs, Outputs and Assumptions for Launch Safety Module

Inputs	Outputs	Assumptions
Missile Dynamics	Launch Noise	Only Weight & Thrust Forces at Launch
Motor Characteristics	100 ft Noise	Constant Motor Thrust & ISP at Launch
	Missile Acceleration	

5   Design of Experiments

The overall goal of the design methodology is to systematically arrive at the best missile that will achieve mission success, while meeting multiple requirements such as weight, noise, and acceleration. The design methodology must also provide understanding as to how each of the design variables impacts the overall design and the constraints, so that trade studies may be conducted. A design of experiments (DoE) approach will meet both of these stated goals because it enables the sampling of the entire design space. It also can be used to build surrogates, and to perform sensitivity analysis. To carry out the analysis four steps are performed. First a broad DoE, with wide variable ranges is completed, allowing the team to explore the entire design space. Based on the results of the broad DoE, the team will perform detailed analysis and configuration down selection. This will allow the team to better meet the requirements. Following the detailed analysis and down selection, multiple refined DoEs are performed with narrow variable ranges. Finally, using the results of the refined DoEs, the team will build surrogate models to optimally size the missile, while meeting the requirements.

5.1   DoE Variables

Using previous missile systems as a starting point, variables for propulsion and geometry are established and assigned upper and lower bounds for input into the DoE. Continuous propulsion variables include the grain fineness ratio, grain outer diameter, grain inner diameter, and maximum expected operating pressure (MEOP). Continuous geometry variables included with airframe are nose fineness ratio, nose bluntness, boat tail length, and boat tail factor. Continuous

ISLAND🏝

variables for the control surfaces include the taper ratio, aspect ratio, leading edge sweep angle, and root chord. The values and their respective ranges are given in Tables 14 through 15 below. In this initial DoE, termed as the broad DoE, a single stage motor configuration is run. The methodology to fill the design space is a Latin Hypercube, which provides good coverage of the interior of the design space.

Table 14: Initial Geometry DOE Ranges

Parameter	Minimum	Maximum
Nose Fineness Ratio	0.5	1.5
Nose Bluntness	0.7	1
Boat Tail Length (in)	1	1.65
Boat Tail Factor	0.9	1
Control Surface TR	0.1	1
Control Surface AR	1	3
LE Sweep (deg)	0	60
Root Chord (in)	1	5

Table 15: Initial Propulsion DOE Ranges

Parameter	Minimum	Maximum
Grain Fineness Ratio	3.3	5
Grain Diameter Ratio	1.9	2.3
Grain Inner Diameter (in)	0.2	0.4
Maximum Expected Operating Pressure (psi)	300	1400

5.2 Broad DoE Outputs

From the large number of input variables defined in the previous section, the environment creates a significant number of outputs, which are detailed in the following section. Overall missile geometry and definition is output in the form of weight, length, and diameter. Results from the trajectory simulation are output as a miss distance to the target. Performance outputs include the load factor from the endgame maneuverability, endgame speed, launch noise, launch acceleration, and the distance traveled by the launch motor.

Each individual case has a unique set of outputs. The statistical analysis and visualization software, JMP, is used to explore the design space with tools such as constellation plots [26]. Such constellation plots are shown in Figures 21 and 22. After applying local data filters, the most feasible designs subject to our constraints emerge. These cases are highlighted in black in the figures. Table 16 outlines the number of cases that meet the each of the requirements. Unfortunately, none of the sampled cases in this initial DoE met the noise, acceleration or maneuverability constraints. Because of this, more detailed analysis and configuration trade studies must be conducted. The Broad DoE proved valuable because it provided a more reduced area of variable ranges where designs would be feasible.
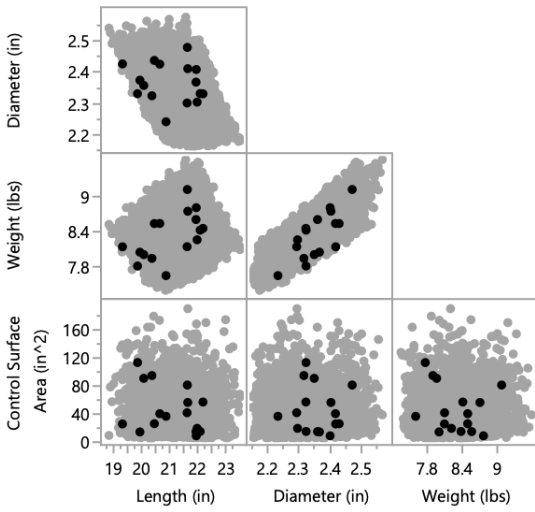
(a) Geometry Scatter Plot
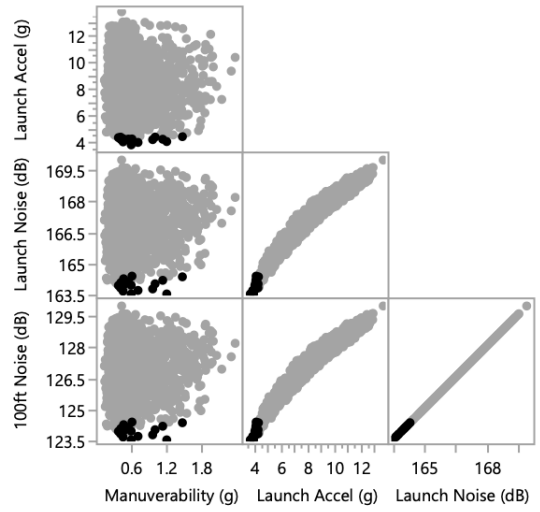
(b) Propulsion Scatter Plot

Figure 21: Discipline Specific Scatter Plot Matrix with Missiles of Interest Highlighted, Broad DoE

ISLAND
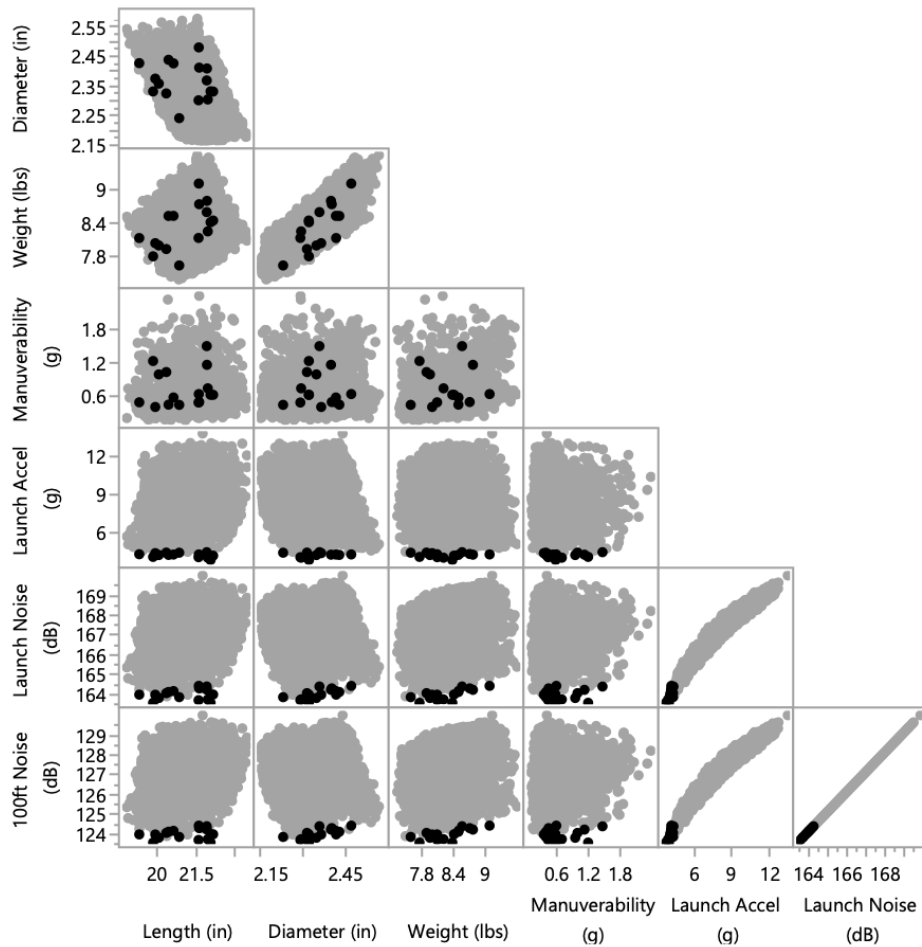
Figure 22: Overall Scatter Plot Matrix, Broad DoE

Table 16: DOE Results Meeting Constraints, Broad DoE

Constraint	Launch Acceleration	100ft Noise	Weight	Hit Target	Maneuverability	Launch Noise
Met	0%	32%	15%	6%	0%	0%

5.3   Trade Studies and Configuration Down Selection

The following subsections outline the experiments and results of the trade studies. These trade studies will allow the team to down select to a final configuration and to better meet the constraints, specifically those that were not met in the initial broad DoE.

5.3.1   Control Surfaces

Control Surface Configuration

To finalize the missile configuration, the surface configuration needed to be determined. Two alternatives were considered, a tail control configuration and a canard control configuration.

In a tail controlled missile, the tail surfaces actuate to stabilize and maneuver the missile. This configuration has poor packaging characteristics due to the interference between the motor casing and the actuators, driving the missile diameter up. Tail control missiles are efficient at high angles of attack but have poor performance at smaller angles.

Conversely, in a canard control design, the tail surfaces are fixed and the missile uses actuating canards for maneuvering. Moving the actuating systems forward alleviates the packaging issues. Opposite to the tail controlled missile, the canard controlled missile has good low angle of attack performance but poor high angle of attack performance.

From preliminary trajectory analysis, as shown in Figure 23, it was observed that the missile spends a large majority of the time at low angles of attack where canards are more efficient.
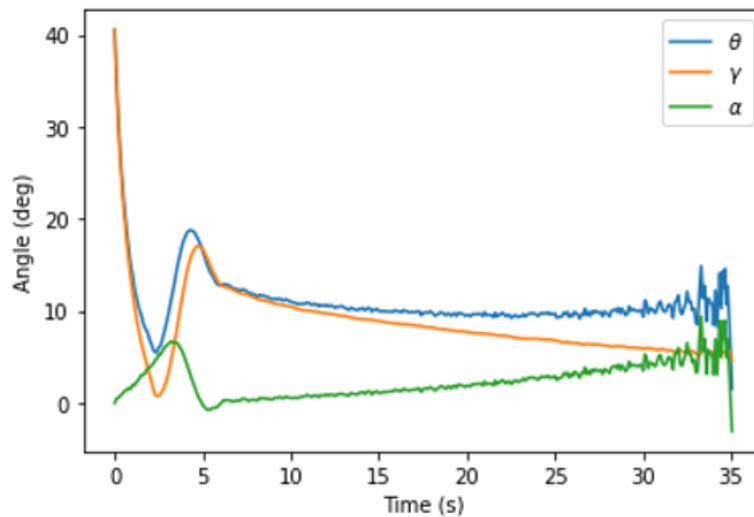
Figure 23: Initial Mission Trajectory Analysis

The maneuverability constraint requires the surfaces to be sized for 6g's of maneuverability. As seen in Figure 24, for a notional missile, the tail surfaces become simply too large to store for a tube launch design if all the surface area was dedicated to the tail.

(a) Canard Control   (b) Tail Control

Figure 24: Canard versus Tail control notional configurations

Based on these findings and observations, canard control was selected.

Control Surface Optimization

The body of the missile is sized directly from the propulsion. It was observed that the feasible designs had very similar body shapes. Locking in a general body size allows for a direct comparison of the surfaces for a missile and a more sensitive analysis of the surface parameters. A DoE was used to design the control surfaces for best performance and to meet maneuverability requirements. To reduce computation time, the analysis was performed within the aerodynamics module for a fixed design condition. A combination of the design variables results in a different trapezoid surface planform. From these ranges, 100,000 cases in the design space were evaluated. Using JMP and the copious design points, surrogate models were generated for maneuverability, surface area, lift-to-drag ratio, and span. Optimization was performed using these surrogate models to meet a maneuverability requirement, minimize surface area to reduce weight, maximize lift-to-drag ratio for efficient flight, and minimize span for efficient storage. Other boundary constraints were added to ensure surface shapes were realistic and were able to be manufactured. The surface parameters produced from the surrogate model optimization were reinforced by running the missile in the full environment to confirm the requirements were met. This process is carried out once to get an initial guess for the refined DoE and is repeated again for the final missile candidates.

5.3.2 Launch Method

There are two major safety constraints that are not met with the baseline missile: the noise limit and the launch acceleration. Additionally, without some type of dedicated launch system, there is a potential for the user to be sprayed by the exhaust gases of the motor. Trade studies are conducted on the launch system configuration that would best meet the launch acceleration, the launch noise and 100 ft noise requirements.

Three launch system configurations are evaluated in this study, as shown in the Discrete Morph Matrix. The first alternative is a two stage integrated launch-flight motor. The launch motor is separated from the flight motor using a burst disk, similar to the Javelin missile system's motor [11]. The launch motor is design to provide the minimum

amount of thrust to maintain a positive rate of climb for 2 seconds, at which point, the flight motor is ignited. This set-up guarantees that the missile does not hit the ground at launch and travels a distance further than 100 feet, before the main motor is ignited. The downside to this system is that it would increase propulsion system design complexity and would still put the crew in danger of exhaust gases since the launch motor will stay lit after exiting the tube. The integrated motor configuration for the Javelin is shown below in Figure 25.
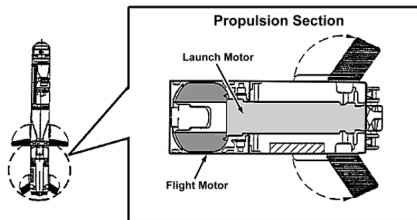
Figure 25: Integrated Launch-Flight Motor for Javelin Missile [11]

The second alternative is an ejectable launch motor. This configuration is similar to that of the Stinger missile and features a motor that is briefly lit while the motor is still in the launch tube. Once outside, the missile would light the flight motor. This system has the benefit of reducing costs and preventing exhaust gas issues, however the crew would still experience the noise from the flight motor and the danger of a projectile. A picture of the ejectable launch motor system for the Stinger missile is shown in Figure 27.

Figure 26: Ejectable Launch Motor for a Stinger Missile [12]

The third and final alternative is a compressed gas launch. This configuration uses compressed gas from a reservoir tank to accelerate the missile out of the tube, before the flight motor is lit. This system has the benefit of preventing exhaust gas issues however, the system has very high maintenance requirements. A picture of the compressed gas launch system, used on a torpedo, is shown in Figure 27.

Figure 27: Compressed Gas Launch for a Torpedo [12]

Integrated Soft Launch

First, a missile with an integrated launch and flight motor was investigated. Using the entire design environment, a properly sized missile with a single stage flight motor is compared to a a properly sized missile with an integrated launch and flight motor. The results of the trade study are shown in Table 17.

Table 17: Integrated Launch Motor vs No Launch Motor

	Weight (lbs)	Launch Acceleration (g)	Launch Noise (dB)	100ft Noise (dB)
Missile Without Soft Launch	9.00	7.36	166	126
Missile With Soft Launch	9.28	2.86	162	122
% Difference	+3.11%	-61.1%	-2.4%	-3.17%

As the table shows, the integrated motor significantly decreases the noise and launch acceleration, at the expense of a slightly increased weight. However, the configuration is unable to meet the launch acceleration or the noise requirements. Thus, further configurations must be analyzed.

Ejectable Soft Launch

The next configuration studied was the soft launch motor. It was designed for a target thrust and burn time calculated from kinematics and the second law. The minimum thrust required to accelerate the missile out of the tube was calculated using Equations 71 and 72. The team assuming a launch tube length of 4ft, constant acceleration of 2g's, a launch angle of 45 degrees, and a missile weight of 10 pounds.

$$V^2_{exit} = V^2_{initial} + 2 * a_{launch} \Delta x_{tube} \tag{71}$$

$$V_{exit} = 22.68 ft/s$$

$$F_{net} = m_{missile} a_{launch} = W * sin(\theta_{launch}) \tag{72}$$

$$T = 27.07 lbf$$

From there, the travel time within the tube, and thus the motor burn time, can be calculated using Equation 73 below.

$$t_{tube} = \frac{V_{exit} - V_{initial}}{a_{launch}}$$

$$t_{tube} = 0.353s$$

(73)

Using the propulsion design environment, a DoE was run. Surrogate models from Neural Nets were created in JMP to design an ejectable motor that meets the previously calculated thrust and and burn time requirements. The results of the study, and the corresponding design parameters are shown Table 18.

Table 18: Results of the Ejectable Soft Launch Study

Design Variables	
MEOP (psi)	105
Grain Diameter (in)	1
Fineness Ratio	1
Inner Diameter Ratio	0.3025
Output Variables	
Average Thrust (lbf)	27
Burn Time (s)	0.35
System Mass (lb)	0.25

In addition to designing a custom motor, the team also investigated commercial off the shelf options that could fulfill the requirements. It was found that the Cesaroni - P29-1G VMAX (F120) motor could meet the requirements with a little modification. The specifications for the Cesaroni are shown below in Table 19.

Table 19: Cesaroni - P29-1G VMAX Design Specifications [27]

Average Thrust (lbf)	26.98
Burn time (s)	0.5
Weight (lb)	0.23
Cost ($)	25

Compressed Gas Launch

The final launch system configuration analyzed was a compressed gas launcher. For this study, it was assumed that the launcher has an expansion tank filled from a high pressure source tank. The system is sized using the launch force and time in tube calculated above. Further sizing assumptions for this trade study are given in the Table 20.

Table 20: Compressed Gas Launcher Sizing Assumptions

Variable	Value
Barrel Diameter	3.5 inches
Barrel Length	48 inches
Missile Mass	9.4 lbs
Expansion Tank Volume	400 in^3

These variables were used in a study that applied pressure to a "plug" at the aft of the missile that was assumed to be the same diameter of the launch tube. The pressure is released from the expansion tank into the launch tube, applying force to the plug and accelerating the missile out of the tube. To determine the final muzzle velocity of the missile, acceleration of the plug is numerically integrated as the compressed gas expands into the tube on an adiabatic basis. Based on the pressure, the launch noise is calculated from first principals. The results are shown in Figure 28.
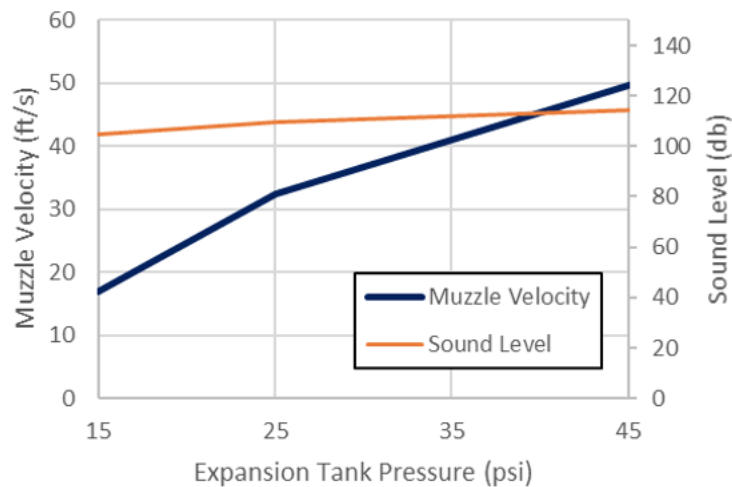
Figure 28: Results of the Compressed Gas Launch Study

While the sizing exercise shows that it would be possible to launch the missile this way, the system would require a heavier launcher, which in turn would drive down the weight of the missile. Also, a high pressure gas source that is capable of meeting the raid scenario of ten expansion tank reloads would be at minimum, 18lbs. There would also be a significant amount of additional equipment, like valves, seals, and hoses, that would require preventative maintenance to ensure successful field operation. Finally, the performance of the system will vary widely with changes in ambient pressure, temperature, and humidity.

Final Propulsion Configuration

Based on the propulsion trade studies, a integrated launch-flight motor configuration is selected. In addition, to

help protect the crew from exhaust gases and to meet the launch acceleration requirement, an ejectable launch motor will be included. To decrease costs, the ejectable motor will be a modified Cesaroni - P29-1G VMAX.

5.3.3 Noise Analysis

From the results of the initial DoE, there is no trade space in which the launch noise is below 120 dB(A). Therefore, the team explored what configuration would meet the noise requirement and potential noise mitigation strategies.

Noise Requirement Feasibility

Two correlations are used to study the noise requirement feasibility. The first correlation, shown in the Approach section in Equation 69, requires the following inputs: motor thrust, specific impulse and distance ratio from user.

The analysis assumes the motor is right next to the user, thus R=1. The minimum thrust required to keep a 10 lb missile off the ground is 10 lbf. The Estes D-12 motor produces approximately 10 lbf of thrust and has a specific impulse of 80 seconds [28]. Using these parameters, it is found that the minimum possible noise at launch, for a missile using a SRM and with a weight of 10 lbs, is 153.3 dB(A). If Equation 69 is rearranged to solve for the distance, given a noise input, it is found that the missile, would need to be ignited 50ft away, at a minimum, so that the user experiences 120 dB(A).

An additional analysis is performed using a different correlation [29] that predicts the noise levels based off peak pressure levels. These relationships are shown in Equations 74 and 75.

$$P_p = \frac{2.3V\sqrt{WD}}{L^2} \tag{74}$$

$$dB(P) = 20log(P_p) \cdot 3.4457 * 10^8 \tag{75}$$

The following assumptions are made: a missile weight (W) of 10 pounds, a missile diameter (D) of 2 inches, a muzzle velocity (V) of 20 ft/s, and a launcher of length (L) 48 in. With these assumptions, the minimum possible noise is 151.26 dB(A). The equations are rearranged to solve for the launch tube length, given a noise requirement. For a requirement of 120 dB(A), the launch tube must be 290 in, or approximately 24 feet long. Even with the muzzle velocity reduced by half, the launcher length would still need to be 200 in or approximately 16.5 feet long.

From these calculations, summarized in Table 21, it is determined that a missile noise limit of 120dB(A) at the launch location is infeasible.

Table 21: Noise Feasibility Analysis Results

Noise Correlation Used	Minimum Noise dB(A)	Requirement to Meet 120 dBA Limit
Correlation 1 [25]	153.5	Missile must be launched 50 ft away from any personnel
Correlation 2 [29]	151.26	Launch Tube Length must be 290 in with 20 ft/s Muzzle Velocity Launch Tube Length must be 200 with 10 ft/s Muzzle Velocity

While 120 dB(A) noise requirement at launch is deemed infeasible, the noise requirement is still an important safety factor to consider, and is treated as a minimization objective. All possible avenues of noise reduction are explored and applied where applicable. To remain consistent with previous noise evaluations, the noise attenuation alternatives are evaluated and applied assuming a frequency of 2500 Hz.

Noise Mitigation Strategies

In terms of noise reduction, the military views mitigation strategies as three-tiered, shown below [30]. The team will outline attenuation methods in each of these areas.

1. Source Reduction

2. Enclosure or other Engineering Controls

3. Personal Protection Equipment (PPE)

The first noise mitigation strategy investigated was source reduction, in the form of nozzle chevrons. Nozzle chevrons, seen in Figure 29, have been used on Commercial aircraft, such as the Boeing 787.
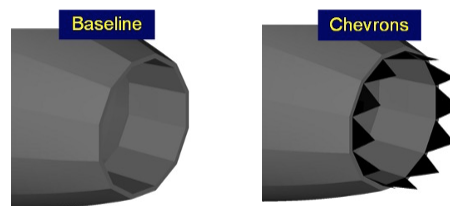
Figure 29: Nozzle Chevrons [31]

Chevrons work by improving the mixing of the jet, and thus lowering the noise, with a small detriment to performance. While initial studied for subsonic exhausts, chevrons offer some noise mitigation for supersonic exhausts, like those that come out of a rocket nozzle. According to Schlinker, the noise level is estimated to drop 2 dB when mod-

erately penetrating chevrons are included [32]. The performance impact is small and is neglected in the preliminary design.

The second mitigation method investigated was an engineering control, in the form of Acoustical Foam on the inner tube of the launcher. POLYDAMP® Acoustical Foam (PAF) is an acoustical grade, open cell, flexible ether-based urethane foam designed to give maximum sound absorption per given thickness while still remaining resistant to heat, moisture, and chemicals while also being hydrolytically stable [33]. Material manufacturers are required by law to publish Material Safety Data Specification (MSDS) sheets that consists of the chemical and physical properties of a particular material. Companies manufacturing materials that target the sound-reduction market often publish sound-reduction coefficients for their materials that represent target individual frequencies [34]. To calculate the decibel drop with a material at a given frequency, the sound-reduction coefficient can be used with the following equation, were d is the decibel drop (dB) and C is the sound-reduction coefficient.

$$d = -20log_{10}(1-C) \tag{76}$$

Equation 76 was used in conjunction with published data for PAF to produce Figure 30 [33]. As seen by the vertical line at 2500 Hz, the approximate noise reduction for 1 and 2 inch foam is approximately 33 and 37 dB, respectively.
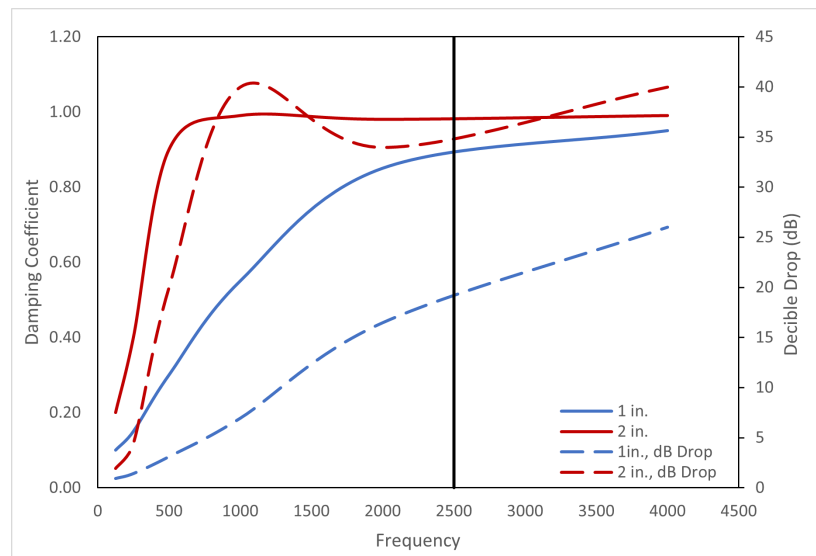
Figure 30: Noise Attenuation of POLYDAMP® Acoustical Foam (PAF) [33]

The third noise mitigation method investigated was Helmholtz Resonators on inner tube of the launcher, again a engineering control. Helmholtz Resonators are small containers, with a narrow throat leading into a larger chamber, shown in Figure 31. The chamber and neck dimensions can be specially designed to have the gas inside oscillate at

a certain frequency, upon excitation. When this occurs, excitation wave, which in this case is a sound pressure wave, will be damped. The damping varies depending on the complexity of the resonator. To minimize cost and complexity, ISLAND will implement a simple set of Helmholtz Resonators inside the launch tube, that will reduce noise by 2 dB [35].
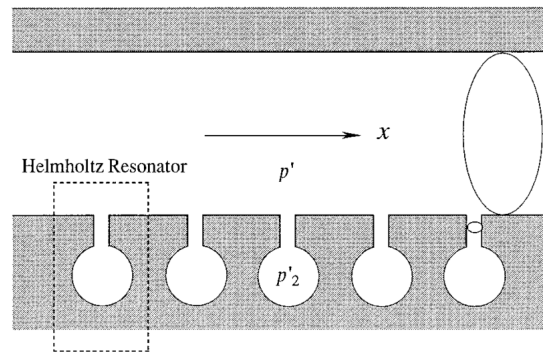
Figure 31: Diagram of Helmholtz Resonators) [33]

The previous methods describe the steps taken to reduce the system noise through source and engineering control methods. With these methods maximized, additional ways to reduce the noise exposure, through the use of PPE, were investigated. The use of hearing protection is standard operational procedure in the military, as described by MIL-STD 1474, with specific design and noise requirements detailed in the most latest publication of MIL-STD-1474E [30].

In a study conducted on the effectiveness of different types of military hearing protection, it was found that for basic hearing protection, meaning passive hearing protection, a combination of earplugs and earmuffs provided the best decibel attenuation. As seen in Figure 32, at approximately 2500 Hz, the noise attenuation is roughly 39 decibels.
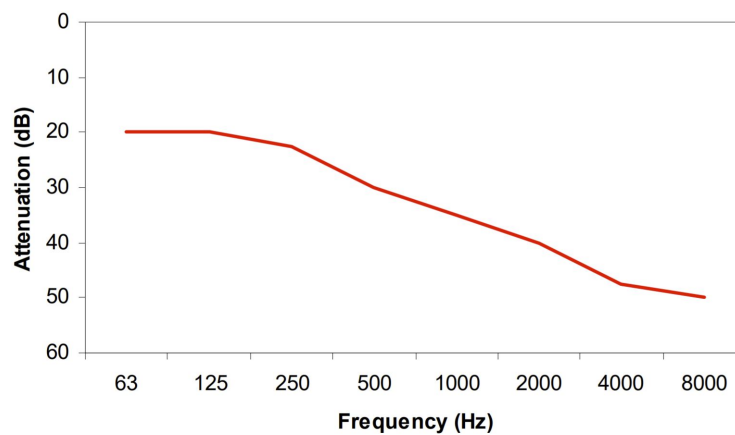
Figure 32: Noise Attenuation when wearing Passive Earplugs & Earmuffs [36]

It should be noted, the 39 decibel drop from PPE does not affect the system noise, with respect to the requirement. Instead, it can be applied after the fact to analyze the user experienced noise and the health hazard it may pose.

Noise Mitigation Results

Figure 33 graphically depicts how each mitigation strategy applied individually would affect the missile system noise or the user-experienced noise. For this figure, the missile noise was derived using the minimum thrust and ISP assumptions from above. This missile still cannot meet the noise requirement, even with the noise attenuation strategies.
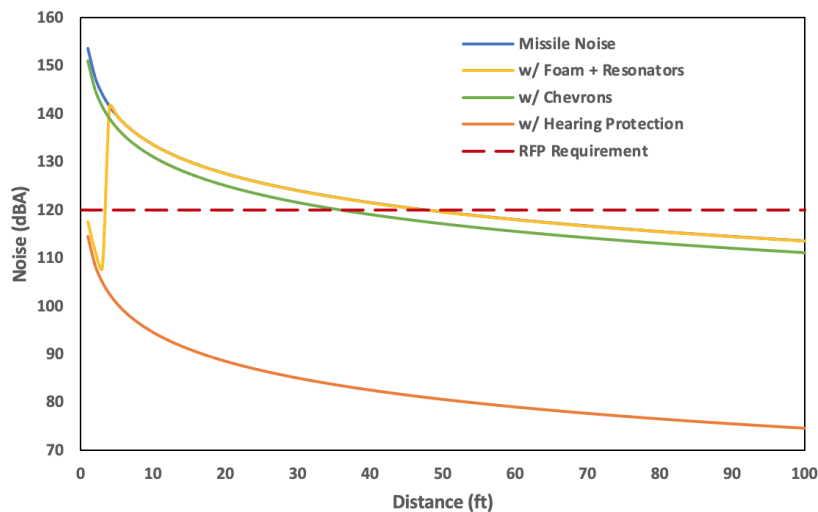
Figure 33: Noise as a function of downrange distance with different mitigation strategies

In conclusion, it is strongly recommended that the ISLAND system incorporate the nozzle chevrons, the acoustical foam, and the Helmholtz resonators it its design. Regardless, the user will need to wear hearing protection to avoid hearing damage.

5.3.4   Seeker and Payload

The seeker and payload are highly coupled subsystems. If the seeker is inaccurate, a larger payload must be designed to accommodate, and vice versa. This trade study section will outline the process of down selecting to a final seeker and payload type as well as determine the required payload mass.

The alternatives analyzed for the seeker are the Ku-Band Semi-Active radar and the autonomous image recognition seeker. The Ku-Band radar offers superior accuracy performance, however it is more expensive and would require an on ground radar source in the form of vehicle mounted, a base installed, or a man portable radar. It has been

successfully used on the Raytheon Coyote [37]. The autonomous image recognition seeker is a mature technology that is used on many autonomous cars. However, this seeker is in its infancy in the missile field, specifically as a targeting system. It poses some technological risk to the program, however it is much cheaper than the Ku-Band radar alternative. It has the downside of lower accuracy.

In terms of the alternatives for the payload, the team considered the impact warhead and the proximity warhead. The impact warhead is simple and cheap, however it requires very high accuracy because the missile needs to physically hit the target. The alternative, the proximity warhead, is slightly more expensive, but does not require as high of accuracy and could be more versatile against different targets.

Seeker Trade Study

The seeker trade study is conducted by performing a Monte Carlo analysis on a fixed missile, by changing a seeker noise factor. The miss distance is recorded for every mission. This factor ranges on a linear scale between 0 and 2, 0 representing no seeker noise, 1 representing a seeker with Ku-Band Semi-Active Radar noise, and 2 representing a seeker with Image Recognition noise. The results are shown in 34.
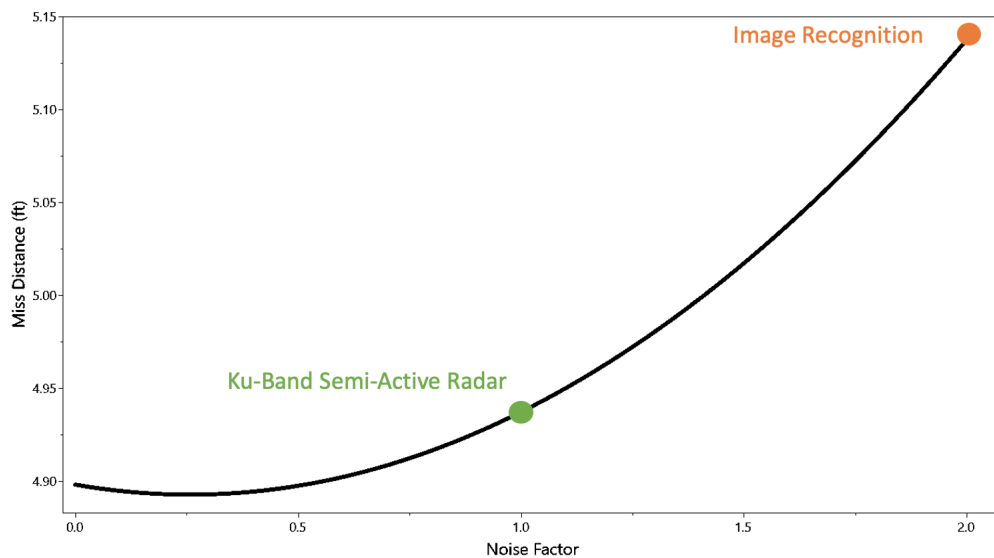
Figure 34: Trade off between Seeker Accuracy and Miss Distance

The figure shows that switching to the less expensive image recognition seeker would only increase the average miss distance by approximately 0.25 feet. This experiment shows the robustness of the Kalman filter and shows that a less expensive seeker would not severely impact miss distance performance. The figure also shows that the missile has a minimum miss distance of 5 feet. This rules out the impact seeker since the missile would be unable to hit

ISLAND

the target consistently. The autonomous image recognition seeker alternative, combined with a proximity warhead configuration, is chosen as the final configuration.

Payload Sizing

The selected payload is a proximity fuse explosive warhead with no fragmentation. Due to the small footprint of the target, and rather fragile structure, it was deemed that a blast warhead would be more effective than a fragmentation warhead. If the missile is used against larger targets, the payload may be switched out for a fragmentation system. First, a required peak overpressure must be identified. As an initial estimate, 3 psi is used. This is the same peak overpressure required to heavily damage parked aircraft [38]. According to Figure 35, the Sea Level kill distance is approximately 11 feet, for a 1 pound blast warhead.
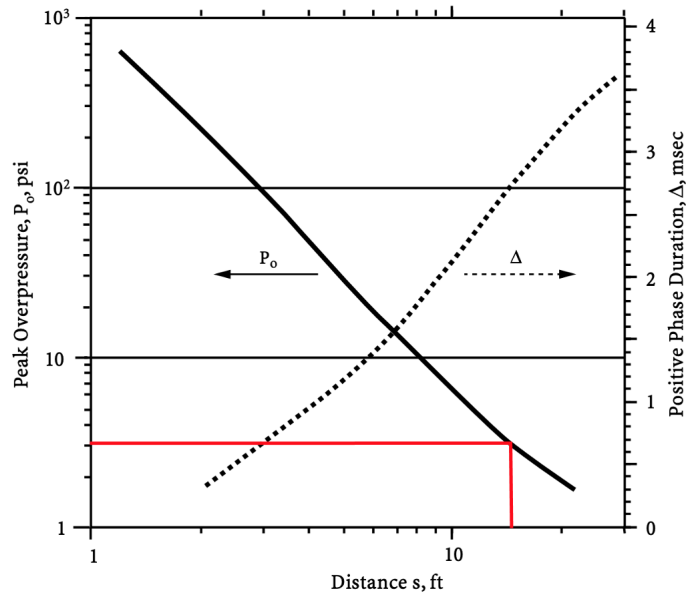
Figure 35: Peak Over pressure verses Distance for 1 lb at Sea Level [39]

A 1 pound warhead is selected. The seeker analysis suggests that this is an oversized warhead, however with this configuration the missile would be more effective against highly maneuverable and larger, armored, targets.

5.4   DoE Refinement

With the completion of the trade studies and utilizing the resulting ranges for successful missile designs from the broad DoE, a refined DoE can be conducted on the final configuration. One DoE is conducted for a missile that meets the threshold performance requirements, range of 3.0 nautical miles and 3,000 feet altitude, and another DoE for a missile

that meets the objective performance requirements, range of 3.4 nautical miles and 5,000 feet altitude.

From the lessons learned in the broad DoE, as well as the trade studies, refined input variable envelopes were identified. These new ranges explore the most interesting parts of the design space. The refined variables parameters for the geometry are shown in Table 22 and the refined propulsion variables are shown in Table 23.

Table 22: Initial Geometry DOE Ranges

Parameter	Minimum	Maximum
Nose Fineness Ratio	0.5	1.5
Nose Bluntness	0.8	1.0
Boat Tail Length (in)	1.0	1.5
Boat Tail Factor	0.9	1.0
Control Surface TR	0.1	1.0
Control Surface AR	1.5	2.5
LE Sweep (deg)	15	40
Root Chord (in)	1.5	2.2

Table 23: Refined Propulsion DOE Ranges

Parameter	Launch Motor		Flight Motor	
	Minimum	Maximum	Minimum	Maximum
Fineness Ratio	1.1	1.3	4.4	5.0
Grain Outer Diameter (in)	1.85	2.1	2.0	2.2
Inner Diameter Ratio	0.63	0.75	0.2	0.4
Maximum Engine Opearting Pressure (psi)	300	400	350	1000

This refined design space allows the team to focus on creating a higher fidelity map of the feasible region. Again, JMP is used to explore the design space. Constellation plots are shown in Figures 36 through 37. These figures display the results for the threshold mission missile. Note that because the ejectable launch motor is part of the configuration, launch acceleration is dropped as a design output. The plots show the distribution of the cases within the design space and how the cases fall relative to other design outputs. After applying local data filters, the most feasible designs subject to our constraints became apparent, and are highlighted in black. Table 24 outlines the number of cases that meet the each of the requirements while also displaying the results of the broad DoE. While most requirements had more successful cases, still, none of the cases met the noise constraint.

(a) Refined Geometry Scatter Plot

(b) Refined Propulsion Scatter Plot
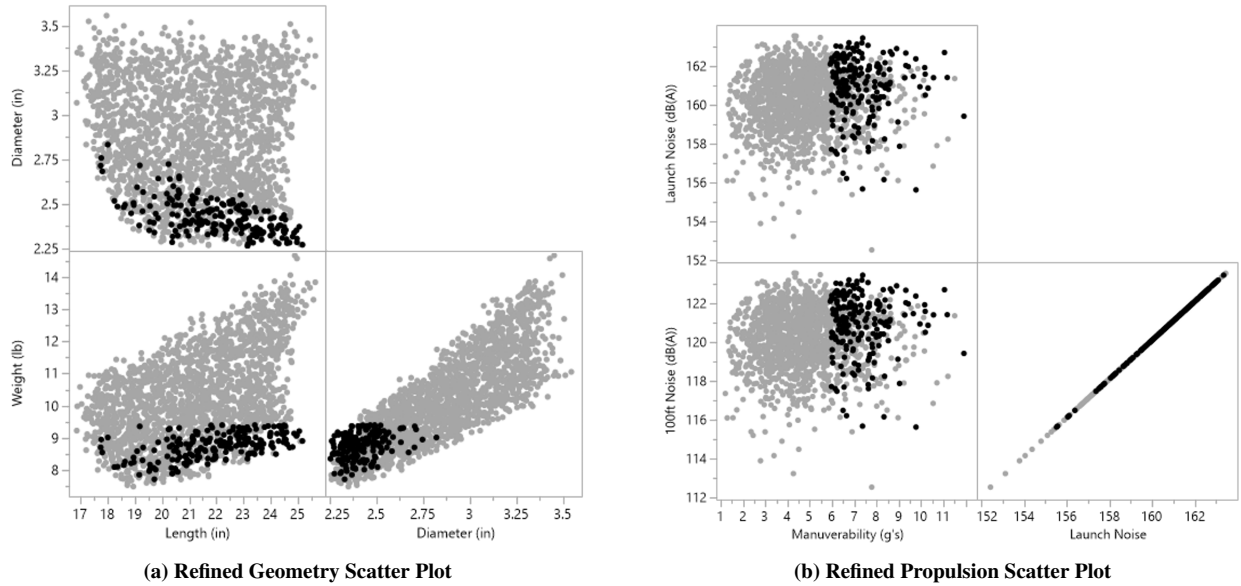
Figure 36: Discipline Specific Scatter Plot Matrix with Missiles of Interest Highlighted, Refined DoE

Table 24: Refined DOE Results Meeting Constraints

Constraint	Launch Acceleration	100ft Noise	Weight	Hit Target	Maneuverability	Launch Noise
Met - Broad DoE	0%	32%	15%	6%	0%	0%
Met - Refined DoE	100%	61%	68%	43%	20%	0%

ISLAND
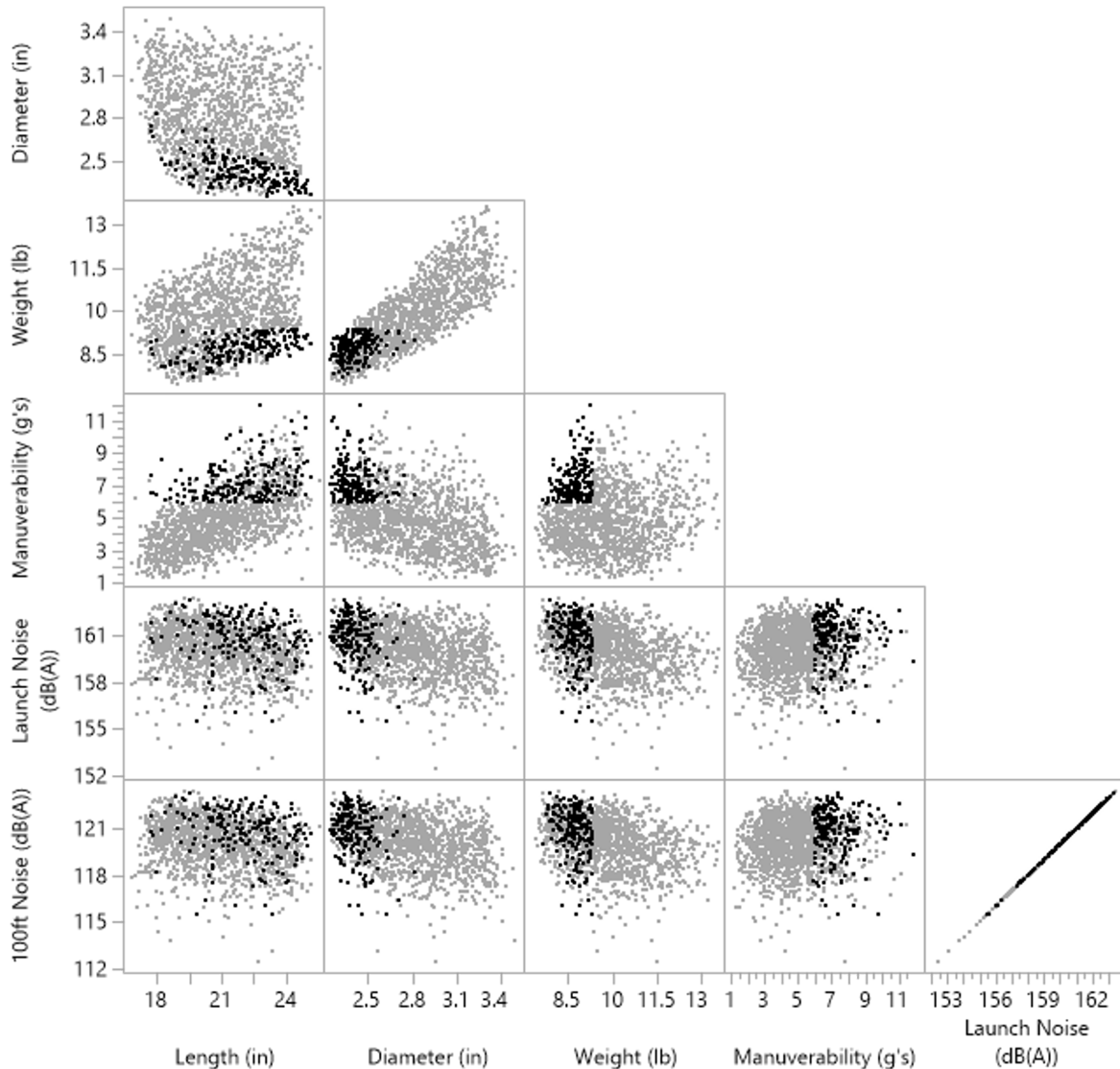
Figure 37: Overall Scatter Plot Matrix, Refined DoE

5.5   Surrogate Modeling

While the results from the DoE are useful, however they they may not contain an optimum solution. The non-continuous variables, like "hit" or "miss", can make interpolation difficult and may cause a good design to be over looked. Surrogate models can be fit using the DoE results to remedy these issues and to better optimize the missile design. Refining the DoE and converging on a final configuration has the benefit of improving the surrogate model goodness of fit.

An optimum solution is one that meets all the requirements and weighs the least. Weight was used as the objective

ISLAND

function because weight is proportional to cost and the goal of the design is to deliver the most cost effective solution, within the constraints.

Using this logic, surrogate models are fit using the results from the two refined DoEs. Specifically, the neural-net functionality in JMP is used to generate the surrogates. Then, optimal missiles for each mission are generated. The missile design from the surrogate is run in the design environment to verify the solution. The metrics for the final missile contenders are shown in Table 25 and respective CAD models are shown in Figure 38. The longer range and higher altitude missile is obviously heavier, larger and produces more noise, compared to its counter-part.

Table 25: Surrogate Model Results for Objective and Threshold Missile

Missile	Diameter (in)	Length (in)	Weight (lb)	Launch Accel (g)	Launch Noise (dB(A))	Maneuv. @ Intercept (g)	Speed @ Intercept (m/s)	Design Range (nm)	Design Altitude (ft)
Objective Mission	2.34	24.30	9.68	2.00	162.66	6.00	145	3.5	5000
Threshold Mission	2.33	20.57	8.43	2.00	161.75	6.00	145	3.0	3000
Advantage	Threshold	Threshold	Threshold	-	Threshold	-	-	Objective	Objective

(a) Optimized Objective Range Design

(b) Optimized Threshold Range Design
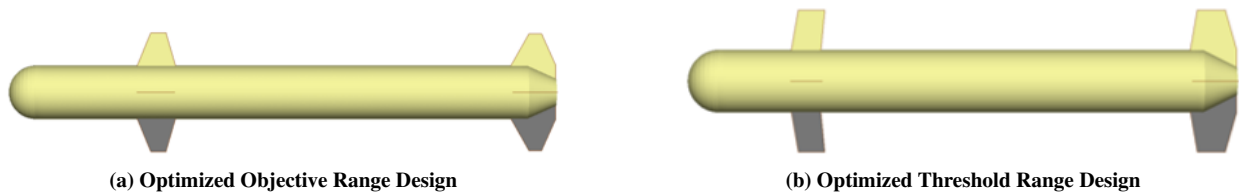
Figure 38: Proposed Designs for the Objective and Threshold Mission Designs

6   Results

This section will outline the detailed design of the ISLAND missile system. The design specifications of the major subsystems will be outlined, as well as information regarding the performance in the design mission, the launcher, the safety performance and the cost and life cycle of the missile system.

6.1   Overall Design

While the threshold range missile is slightly quieter and would allow a squad to carry an extra missile, the capability of the objective mission design outweighs these concerns. Therefore, the final missile design is the objective mission missile. It has the following configuration: canard control, a two stage solid rocket motor to lower noise, an ejectable soft launch to prevent user exposure from exhaust gas and to minimize launch acceleration, and a proximity fuse with

an autonomous image recognition as the primary seeker. There is capability for the seeker to be changed out to a semi-active or active radar, depending on mission needs. The performance metrics for the final missile are shown in Table 26. Using a set engine deck and more accurate mass calculations, an updated CG location was generated. Accounting for the new CG location, the control surfaces were optimized again using the method previously described. A CAD model of the final missile is shown in Figure 39.

Table 26: Final Missile Results

Missile	Weight (lb)	Launch Accel (g)	Launch Noise (dB(A))	Maneuv. @ Intercept (g)	Speed @ Intercept (m/s)	Design Range (nm)	Design Altitude (ft)
ASDL ISLAND	9.68	2.00	162.66	6.00	145	3.5	5000
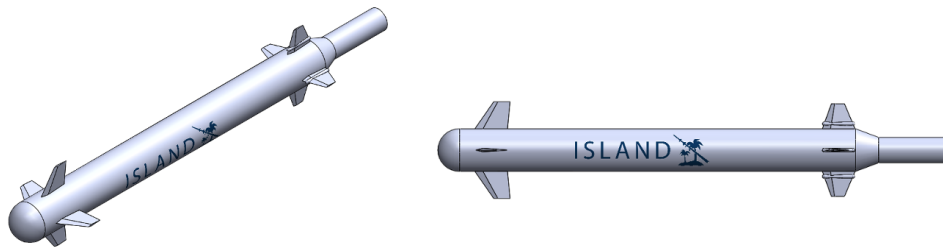
Figure 39: ISLAND 3D CAD Rendering

The body design geometry parameters are shown in Table 27. The length and fineness variables incorporate the nose and boat tail lengths, but do not consider the ejectable launch motor.

Table 27: ISLAND Body Design Results

Body Variable	Value
Body Diameter (in)	2.34
Body Length (in)	24.30
Body Fineness Ratio	10.37
Nose Fineness	1.45
Nose Bluntness Factor	1
Boat Tail Diameter (in)	1.07
Boat Tail Length (in)	1.3
Ejectable Motor Diameter (in)	1.07
Ejectable Motor Length (in)	4.0

6.2   Missile Weight, Subsystems and Center of Gravity

One of the design objectives of ISLAND was to minimize cost, and thus weight. The ISLAND subsystem weights are calculated according to the relationships described in the Approach section. Additionally, the center of gravity for

each important subsystem is identified and measured. This allowed the team to identify the missile CG in different phases of the mission, to determine the stability. The weight and center of gravity breakdown is shown in Table 28. The subsystem and center of gravity diagram is shown in Figure 40.

Table 28: ISLAND Subsystem Weight Breakdown

Subsystem	Weight (lb)	Center of Gravity (in from nose)
Canard Surfaces	0.06	2.96
Guidance, Navigation and Control	3.84	4.88
Payload	1.00	10.03
Flight Motor Propellant	1.72	15.44
Flight & Launch Motor Structure	2.38	17.11
Launch Motor Propellant	0.33	21.60
Tail Surfaces	0.04	22.00
Ejectable Motor Propellant & Structure	0.30	25.21
Missile before launch	9.67	11.60
Missile w/o ejectable motor	9.37	11.12
Missile after burnout	7.32	9.64

1. Canard Surfaces CoM
2. GNC CoM
3. Vehicle CoM @ Burnout
4. Payload CoM
5. Vehicle CoM w/o Ejectable motor
6. Vehicle CoM before Launch

7. Flight Motor CoM
8. Propulsion Structure CoM
9. Launch Motor CoM
10. Tail Surfaces CoM
11. Ejectable Motor CoM

Figure 40: Subsystem Layout and Missile Center of Mass Breakdown

The center of gravity translates approximately two inches throughout the mission due to propellant consumption. The effects on the missile stability will be discussed below.

6.3   Structures and Manufacturing

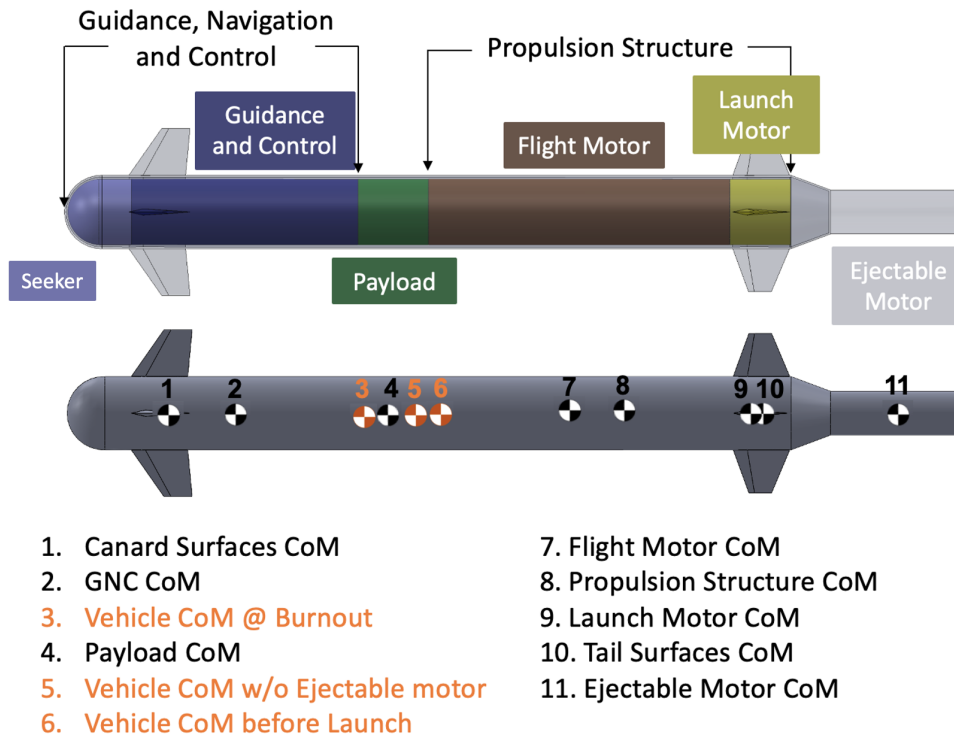The predicted loads from the trajectory are used to arrive at structural thickness values for the missile airframe and casings for both motors as was defined in the approach. Aluminum 2219 was used for the airframe and alloy steel 4130 is used for the motor casings. The results from the thickness calculations are detailed in Table 29.

Table 29: Structural Thickness Sizing for ISLAND

Thickness	Airframe (in)	Launch Motor Case (in)	Flight Motor Case (in)
Manufacturing	0.0162	0.0112	0.0113
Thrust Loading	0.0008	0.0006	0.0006
Bending Loading	0.0117	0.0078	0.0078
Buckling, bending	0.0202	0.0097	0.0095
Buckling, compression	0.0279	0.0134	0.0131
Internal Pressure	N/A	0.0083	0.0292
Final RSS Value	**0.0400**	**0.0230**	**0.0361**

From these results it is seen that the airframe is sensitive to bending. Any additions to bending loading on the missile, e.g increased g loading will need to be evaluated in development.

The motor case is limited in resisting the internal motor pressure. The motor casing is designed to carry both the launch and the flight motor in a combined piece and the casing is designed for the peak pressure of the main flight motor, 1,050 psi. With the goals of minimizing cost, complexity, and weight, the missile design will go forward with 0.038 inch seamless drawn tubing for the cylindrical portions of the motor casing. The forward and end cap portions of the motor casings are formed from the same thickness steel material via machining from billet or formed from sheet steel. The propellant casing will be modular and can be stored away from the airframe. The casing will be secured in place by a forward bulkhead and the aft boat tail. It is assumed the third party motor casing for the ejectable motor is properly designed for development.

6.4   Aerodynamics

As discussed in the Design of Experiments, a canard controlled configuration was selected because the missile spends a majority of the mission at low angle of attack and will allow for more efficient packaging. A diamond airfoil is selected because the missile spends a non-insignificant portion of the mission in the transonic regime. The rest of the surface design parameters are optimized according to the methodology in the Design of Experiments section. The final design parameters, and subsequent surface variables are shown in Table 30. The surfaces are visually represented in Figure 41.

Table 30: ISLAND Aerodynamic Surface Design Results

DOE Design Variables	Canard	Tail
Number of Surfaces	4	4
Taper Ratio	0.5	0.4
Aspect Ratio	2.20	2.18
Leading Edge Sweep (deg)	35	20
Root Chord (in)	1.8	1.8
Additional Geometry Variables	**Canard**	**Tail**
Location of Leading Edge From Nose (in)	2.04	21.21
Half Span (in)	1.49	1.37
Tip Chord (in)	0.90	0.72
Leading Edge Thickness angle (deg)	25	25
Location of Max Thickness (% chord)	0.25	0.25

The aerodynamic drag polars for the ISLAND system are shown below in Figure 42. There is a clear drag rise in the transonic regime, as expected. The jump is attributed to the step-wise correlations as a result of the body build-up method described by Fleeman. Future work could focus on using higher fidelity programs like Missile DATCOM and Star-CCM+.

(a) Canard Surface Drawing   (b) Tail Surface Drawing
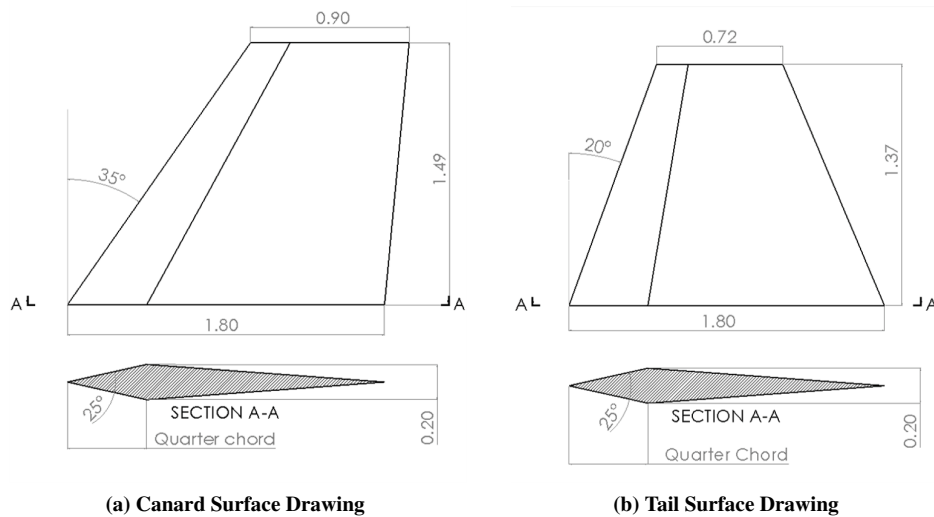
Figure 41: 3D CAD drawings of the surfaces
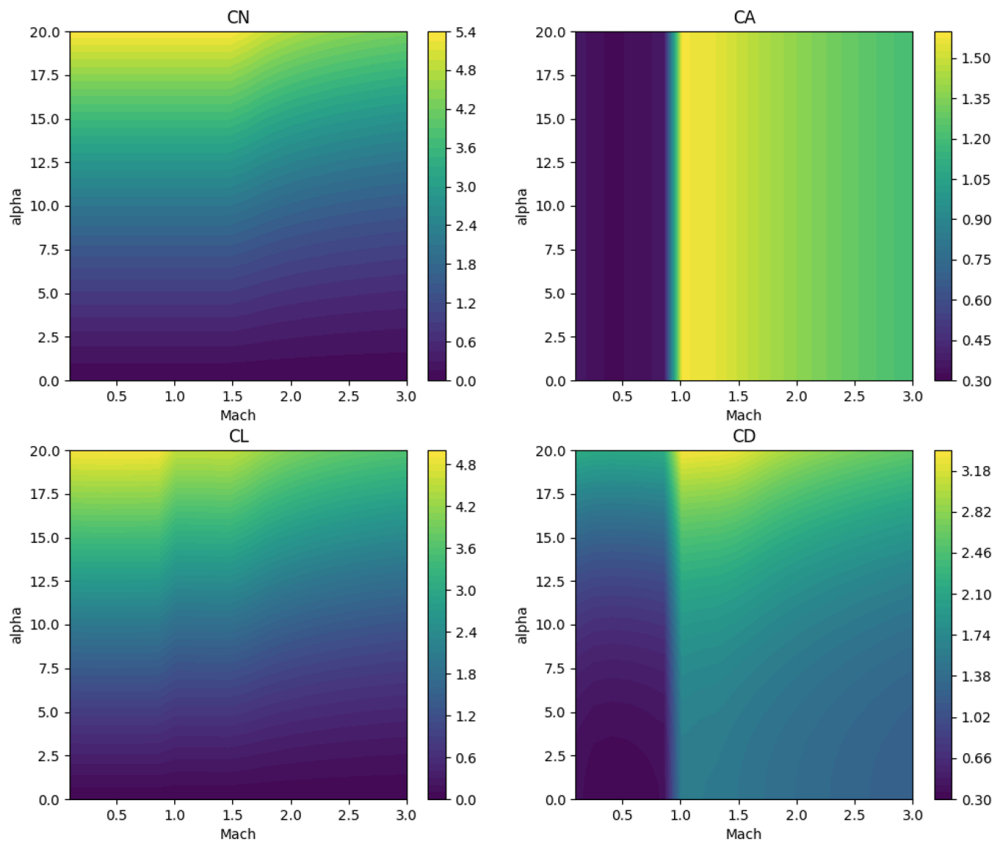
Figure 42: Aerodynamic Polars for ISLAND

6.5   Stability

A stability analysis of the missile is important to understand its performance. A missile with a positive static margin will return to its original angle of attack after a disturbance, without intervention. A statically stable missile will have the center of gravity forward of the center of pressure. A missile cannot be too stable, otherwise it will be difficult to control and will have poor maneuverability [15].

When sizing the aerodynamic surfaces for ISLAND, a stability trade-off was considered. One option was to size the surfaces so that the center of pressure was behind the center of gravity for the entire mission. Because the CG moves forward as propellant is burned, the missile would become overly stable in the endgame, hurting the maneuverability. Thus it was decided to size the surfaces for a center of pressure at 40% length from the missile nose. This would result in an negative static margin condition at launch, and a slightly positive static margin in the endgame. This will require a high bandwidth control system to maintain the missile stability.

The static margin and the required canard deflection is calculated for both the launch and the burnout conditions.

A 3 degree AoA is assumed. The results are shown in Table 31. Even in the most unstable condition, the canard deflection to maintain 3 degrees AoA is small.

Table 31: Static Margin and Required Trim Angle for Different Design Conditions

Condition	Center of Gravity from Nose (in)	Center of Pressure from Nose (in)	Static Margin (%)	Canard Trim Angle (°)
Launch	10.94	9.72	-52.1	-1.01
Motor Burn Out	9.62	9.72	4.2	0.15

6.6 Propulsion

As discussed in the launch system trade study, the ISLAND system will feature a two stage integrated launch-flight motor and an ejectable launch motor. This unique configuration will allow ISLAND to minimize noise, meet acceleration, and minimize crew safety risk from the exhaust gases. The ejectable launch motor is the Cessaroni P29-1G with Vmax propellant to save costs.

The ejectable launch motor will fire for about 0.3 seconds to allow the missile to leave the tube. After this point, it will stop and separate itself from the airframe using a ejection charge. Then, the launch motor will fire for approximately 3 seconds. The launch motor is specially designed for low noise operation. After the launch motor burns out, the flight motor engages and gives the missile enough energy to complete the mission.

Characteristics of all 3 motors are shown below in Table 32 and a cross section of the grains for the integrated motor is shown in Figure 43.

Table 32: ISLAND Propulsion System Design Parameters

Parameter	Cessaroni P29-1G Vmax	Launch Motor	Flight Motor
MEOP (psi)	105 (est)	215	1050
Grain Outer Diameter (in)	1.14	2.10	2.05
Fineness Ratio	3.30	1.35	4.55
Grain Length	3.76	2.84	9.33
Inner Diameter Ratio	0.30 (est)	0.63	0.20
Inner Diameter (in)	0.34 (est)	1.32	0.41
Propellant Type	Cessaroni Vmax	APCP	APCP
Grain Type	BATES	BATES	BATES

The propellant grains are all stable for long term storage. Thus the propulsion system design meets the 10 year, no maintenance requirement.

(a) Launch Motor   (b) Flight Motor
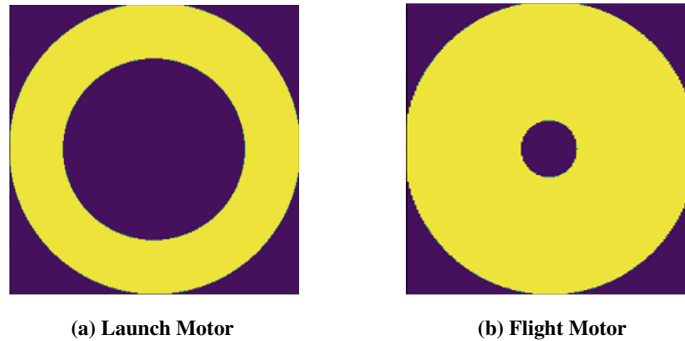
Figure 43: Grain Cross Sections of the Integrated Launch-Flight Motor

The flight and launch motor share similar enough outer diameters to where the casing can be a single diameter and no filler material will be needed. The unknown values for the Cessaroni P29-1G motor are estimated using the results from the custom ejectable launch motor sizing experiment.

The performance plots of the integrated launch-flight motor are shown in Figure 44. The results are expected for a BATES type grain.

(a) Thrust verses Time

(b) M-dot verses Time

(c) Chamber Pressure verses Time Design Mission
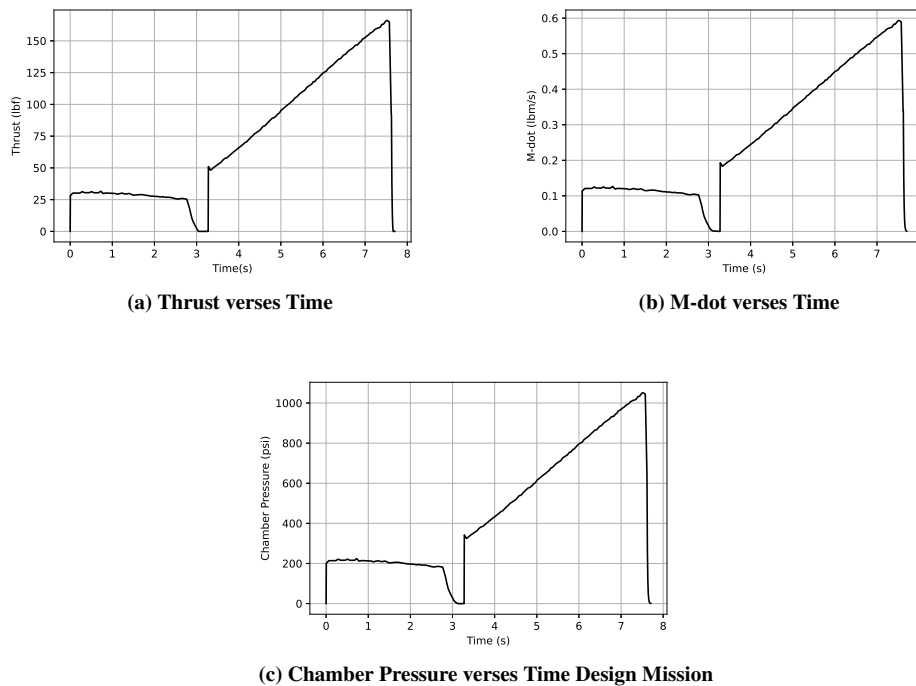
Figure 44: Integrated Motor Performance Plots

6.7 Trajectory

To ensure that the missile meets the performance requirements, the missile trajectory is analyzed. The performance against different types of maneuvering targets is also analyzed.

The first plots analyzed were the range, altitude and trajectory plots, shown in 45. These plots show how the missile first prioritizes getting away from the user, to minimize noise, before climbing to engage the target. The trajectory plots, Figure 45c, shows the 3 types of guidance as well.
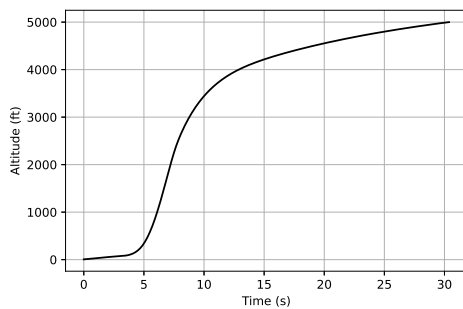
(a) **Altitude verses Time Design Mission**
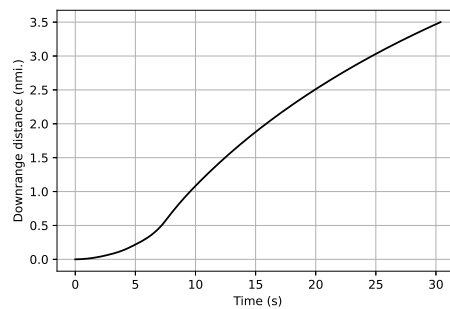
(b) **Range verses Time Design Mission**
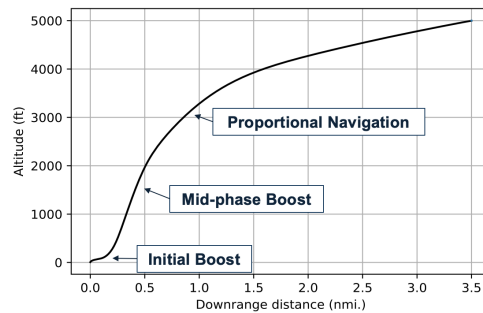
(c) **Trajectory Design Mission**

Figure 45: Range, Altitude and Trajectory Plots for Design Mission

The next plots analyzed were the flight angle and forces, shown in Figure 46. These angle plot shows how the noise in the sensors affects the commanded angle of attack. The missile forces show how the missile begins to turn towards the target, and how that change effects drag.

(a) Missile Flight Angles verses Time

(b) Missile Forces verses Time
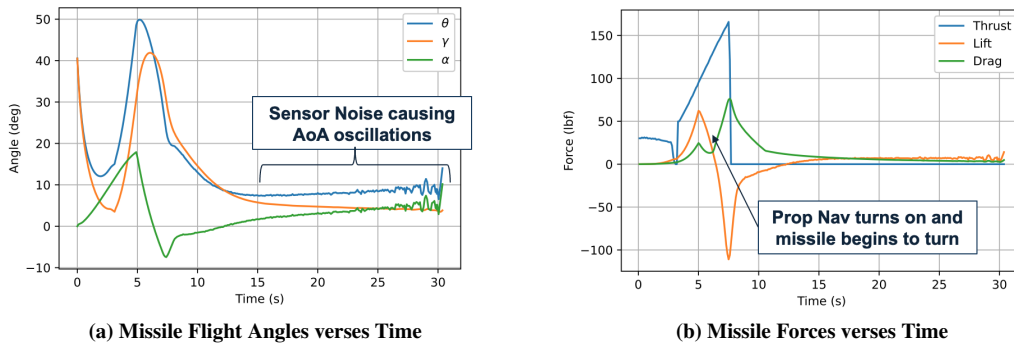
Figure 46: Forces and Flight Angles Plots for Design Mission

The final mission plots analyzed were the missile speed, Mach Number and mass verses time, shown in Figure 47. The plots show that the max speed of the missile is 1.43 Mach and the intercept speed is 0.43 Mach. There are distinct kinks in the plots showing launch motor burnout and flight motor burnout.

(a) Speed verses Time

(b) Mach Number verses Time

(c) Mass verses Time Design Mission
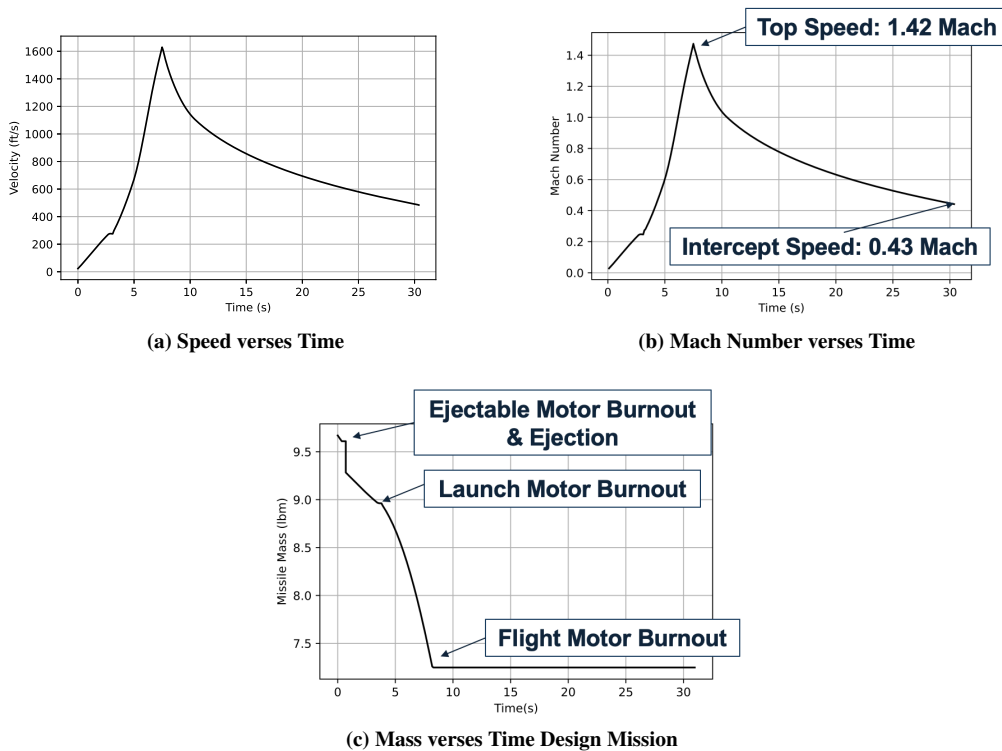
Figure 47: Speed and Mass Plots for Design Mission

The final trajectory analysis performed was to test the missile against different types of targets. For the design

mission, 3.5 nmi. range and 5,000 feet altitude, the target is directed to maneuver with a certain magnitude, to a certain angle, when the missile is within 1000 ft. Then, the miss distance is measured.

Based on this methodology, a Monte Carlo Analysis is conducted, randomly varying the maneuver angle and magnitude. Using a kill radius of 11 feet, the probability of a hit can be determined. The results are shown in Figure 48. The figure shows good performance with targets who have accelerations less than 1.50 g's. Interestingly, the analysis shows a higher probability of hits for targets who maneuver upwards. The hit probability can be further improved if the target is closer, if the missile moves faster at intercept, or if the target maneuvers later.
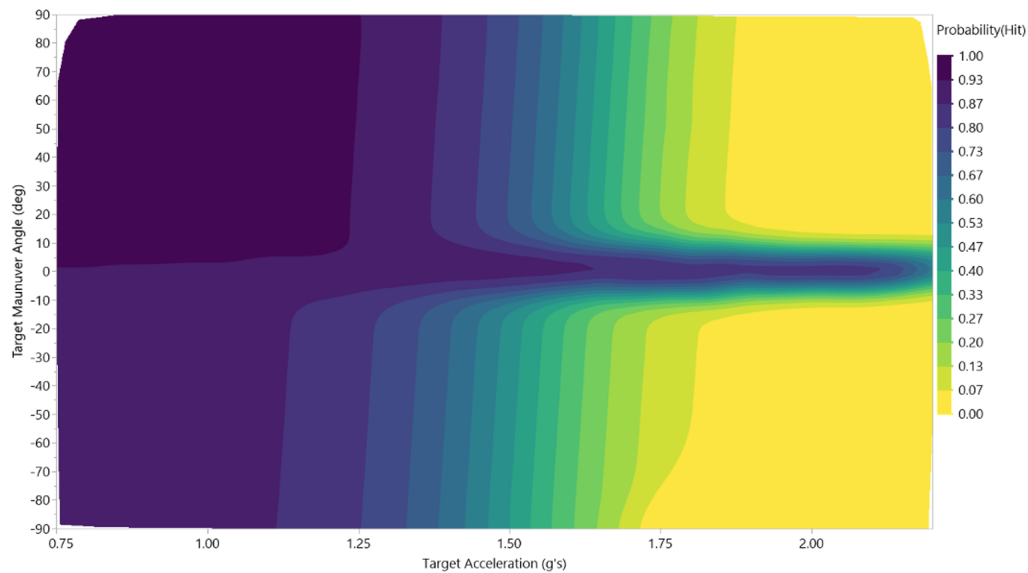
Figure 48: Miss distance verses target acceleration and maneuver angle for the design mission.

6.8   Launcher

The ISLAND missile is designed to be shoulder launched from a circular tube. To reduce the required launcher tube size and weight, a fin folding scheme was developed. The tail fins were designed to fold to reduce overall diameter but not be a constraint in sizing of the aft motor or nozzle. The forward fins will be stowed in a partial switchblade design, where a spring loaded pivot will automatically deploy as the missile leaves the launch tube. The canard and tail deployment methods are illustrated in Figure 49. This method of fin storage is proven as an effective deployment system in use on the Thales Lightweight Multirole Missile (LMM). This design has advantages as that it can simply be loaded by a fire team member from the aft of the launcher, and the forward fins will partially stow as the launcher is loaded, and the tension in the switchblade design will center the missile for launch.

Partial Switchblade

Folded
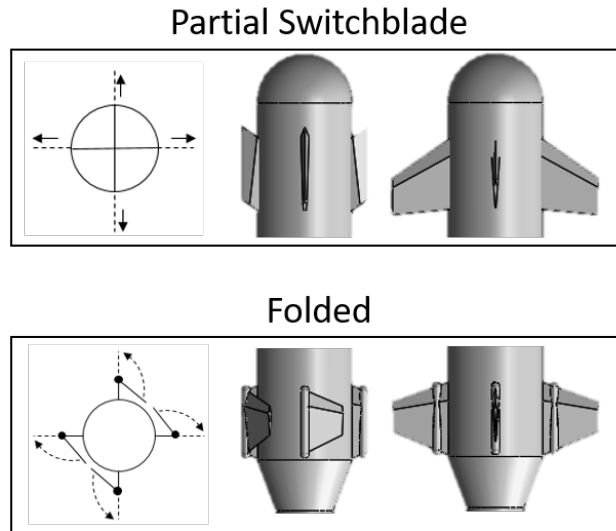
Figure 49: Fin Storage and Folding for Launch Design

The launcher design was initially derived from the FIM-92 Stinger missile shoulder launch system. Acoustic foam and Helmholtz resonators within the interior of the launch tube will be used to reduce the noise produced at launch. Aluminium tubing is selected and sized to incorporate noise reduction and a folded missile. As discussed in seeker system trade study, the selection was made to use an image recognition system as the missile's seeker. With this type of seeker, the missile will be fire and forget, thus eliminating a need for direct optical tracking with the launcher. The launcher will however, be capable of displaying the seeker's imaging to assist in target assessment to determine threat level, engagement successes, and gathering of additional intelligence. After applying noise reduction foam to the launch tube and applicable electronics, the launcher took shape as shown in Figure 50.
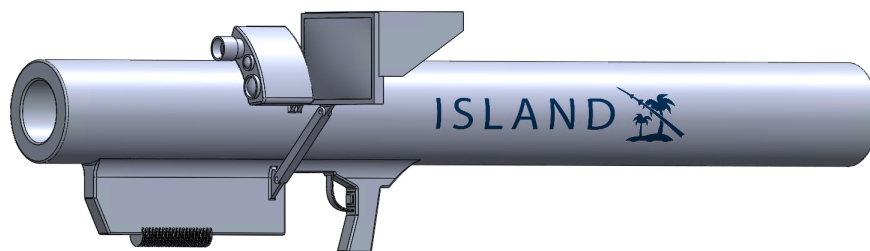
Figure 50: Final ISLAND Shoulder Launcher

The launch and loading procedure will be defined as follows. The gunner will engage the launch safety activation and forward stop. This prevents launch and physically restricts the missile from sliding too far forward. A second team member will load the missile in the aft end of the tube. Once fully loaded, the aft stop will be engaged to

physically stop the missile from sliding backwards. Next, the gunner will receive the signal to activate the missile to engage contacts for firing the ejectable motor. From this point the gunner is free to engage targets with the direction of the communications officer. The triggering sequence will be a "safety off" to disengage the forward stop and then engaging the trigger to light the ejectable motor for launch. This cycle can be completed effectively within the six minute timeframe required for the swarm scenario provided in the RFP. The final dimensions for the system are given in Table 33.

Table 33: ISLAND Shoulder Launcher Dimensions

Variable	Value
Inner Diameter (in)	3.1
Outer Diameter (in)	5.1
Length (in)	48.0
Weight (lbs)	25.3
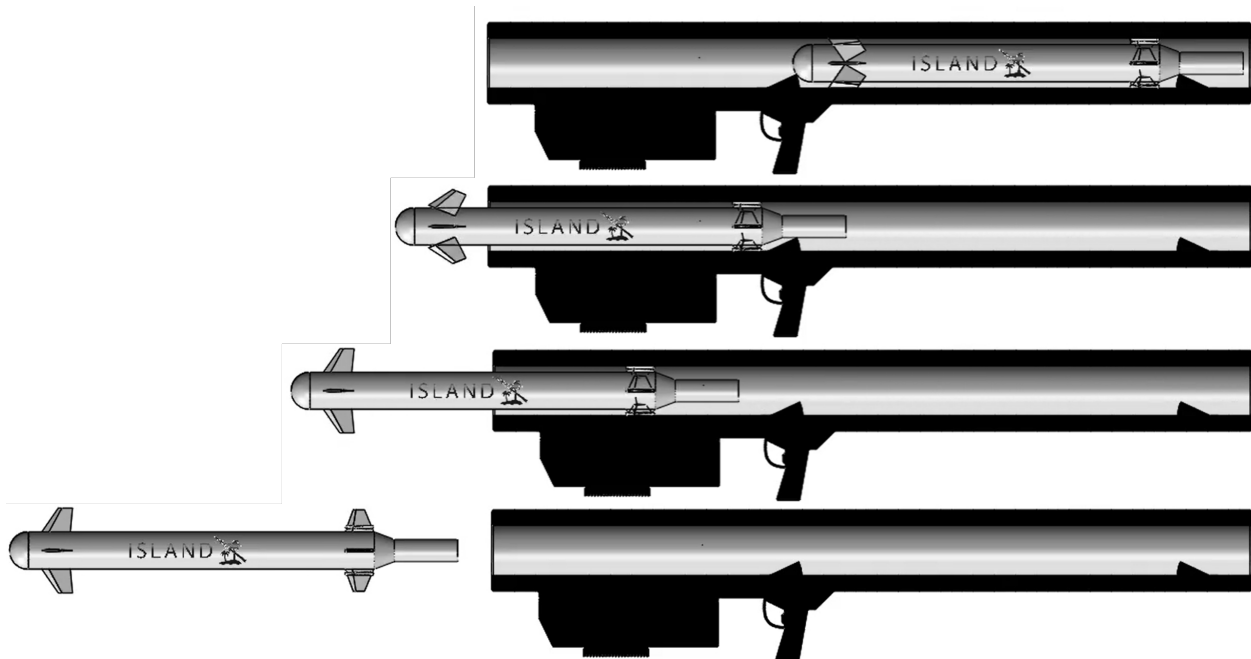
Figure 51: Launch Sequence with Fins Unfolding

In order to meet the one hour raid requirement, the user will have to reload, detect the next target and launch the missile within 6 minutes. For the initial ISLAND design, the payload is not interchangeable, thus the missile can be directly reloaded.Without physical testing, it is difficult to measure an exact reload and reengage time. Therefore, the reload time and re-engagement time for the ISLAND missile is estimated based on past systems. The Javelin Shoulder Launched missile does not have a interchangeable payload and is able to reload and engage 3 targets within 3 minutes

[11]. Therefore, as a conservative estimate, it is assumed that the ISLAND reload and engage time is 2 minutes.

6.9   Safety

The safety of a shoulder launched system is multi-faceted. In terms of the RFP requirements, there are 3 major considerations: warhead safety, launch acceleration and launch noise. The team also considered the launch exhaust impact during the design.

In terms of warhead safety, the choice of a proximity fuse warhead guarantees that ISLAND can be programmed with a minimum arming distance of 200 feet, as calculated by the on-board sensor.

In terms of the launch acceleration and the launch exhaust, ISLAND meets these requirements by incorporating an ejectable soft launch motor in its configuration. This motor, if sized to the burn time and thrust specifications outlined in Section 5, will allow ISLAND to meet the launch acceleration and exhaust requirement.
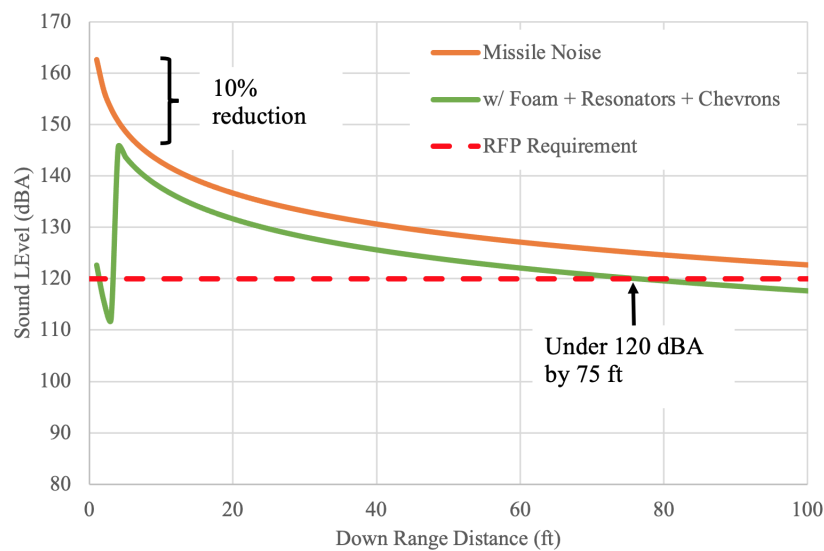
Figure 52: ISLAND Noise as a Function of Distance, with Noise Mitigation

To compare to historical noise levels of currently in-service military weapons systems, the missile noise with noise attenuation from the nozzle chevrons was calculated. The ISLAND missile noise falls at 160 dB(P), as seen in Table 34, which falls on the lower end of noise levels for current missile systems. This comparison is done without the mitigation measures from the launcher, which drop the maximum noise a further 12 dB within 3 feet of the launch location.

ISLAND

Weapon	Model	Firing Condition	Noise Measurement Location	Sound Level (dBP)
Machine Gun	MK19, Mod 3	Fired from HMMWV	Gunner	145
0.50 Caliber Machine Gun	M2	Fired from HMMWV	Gunner	153
7.62mm Machine Gun	M60	Fired from HMMWV	Gunner	155
9mm Pistol	M9	—	Shooter	157
5.56mm Squad Automatic Weapon	M249	Fired from HMMWV	Gunner	160
ISLAND Anti-UAV Missile	–	–	Gunner	160
Javelin Antitank Missile	–	Open Position	Gunner	160
Grenade	M26	–	at 50ft	164
Stinger Missile	FIM-92A	–	Gunner	165
Javelin Antitank Missile	–	Enclosed Position	Gunner	166
Javelin Antitank Missile	–	Fighting Position	Gunner	172
150mm Towed Howitzer	M189	Firing M203 Propellant	Gunner	178
Light Antitank Weapon	M72A3	–	Gunner	182
105 Towed Howitzer	M19	At Charge 8	Gunner	183
MAAWS Recoiless Rifle	M3	–	Gunner	190

6.10 Cost, Development and Life Cycle

The overall goal of the ISLAND system is to provide a low-cost solution to destroy Type 1 and Type 2 UAVs. A missile can be very capable, however if it costs too much, it may not be the right tool. Thus, the following subsections will outline the unit, development and life cycle costs.

6.10.1 Missile Cost

Using the cost correlation described in the approach section, and the final missile weight of 9.68 pounds, the 1000th missile cost is calculated to be 33,000 in 1999 USD. Adjusting to 2020 dollars, the 1000th missile cost is 53,000 USD.

Analysis into the correlation suggests that it is overly conservative for the ISLAND design. The only similarly sized missile in the correlation is the Javelin missile system . The Javelin system utilizes higher tech features, such as thrust vectoring control, which drive up its per missile cost [15]. As an additional data point, the Stinger missile system, which serves as a viable benchmark, comes in at a per munition cost of 38,000 USD [12]. While the Stinger can be applied to our RFP mission, it has a cost that exceeds the target to meet RFP requirements. Considering the development of ISLAND compared to similarly sized man portable missile defense systems, the following cost reductions are assumed, shown in Table 35.

Table 35: Table of Assumptions for Cost Reduction

Subsystem	Assumption
Materials	10% reduction for using commonly available materials
Seeker	10% reduction for using a low cost seeker alternative
Warhead	10% reduction for using low-cost blast warhead
Manufacturing	10% reduction due to low part count [15]

These assumptions result in a per missile cost of $35,400 in 2021 USD for the 1,000th missile. Based on a learning curve of 0.8, seen in Figure 53, the ISLAND system will reach $28,000 per unit when the last missile in the block is completed, well under the Stinger missile. The total cost of the 2000 missiles is approximately 70 million.
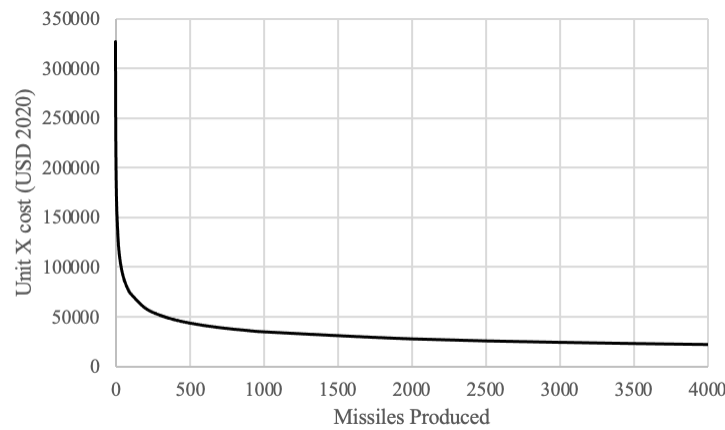
Figure 53: ISLAND Production Learning Curve

6.10.2   Development Costs

A notional development plan is created for the ISLAND system and is shown in Figure 54. Based on the development plan length and the correlation from the approach section, the total development cost of the ISLAND is estimated at 722 million USD, in 2021 dollars. Table 36 gives the development costs of tactical missiles of various applications.

Table 36: Development Costs for Past Tactical Missiles [15]

Missile System	1999 MM USD (millions)	2021 USD (millions)	Program Description
TOW 2	68	108	Wire guided anti-tank
LB Hellfire	392	623	Air to ground anti-tank
Hellfire II	153	253	Air to ground anti-tank
ESSM (SeaSparrow)	247	393	Ship based anti-aircraft
Javelin	708	1,126	MANPAD anti-tank

Compared to these values, the development cost cited is high but is difficult to accurately predict given the limited amount of public data available for man portable anti-aircraft systems. In addition to development costs, the a notional

development plan for ISLAND is proposed in fig54 below. The plan walks through conceptual, preliminary, and detailed design phases as well as identifying prototyping, testing, and field trials to arrive at a final IOC date at the end of 2027.
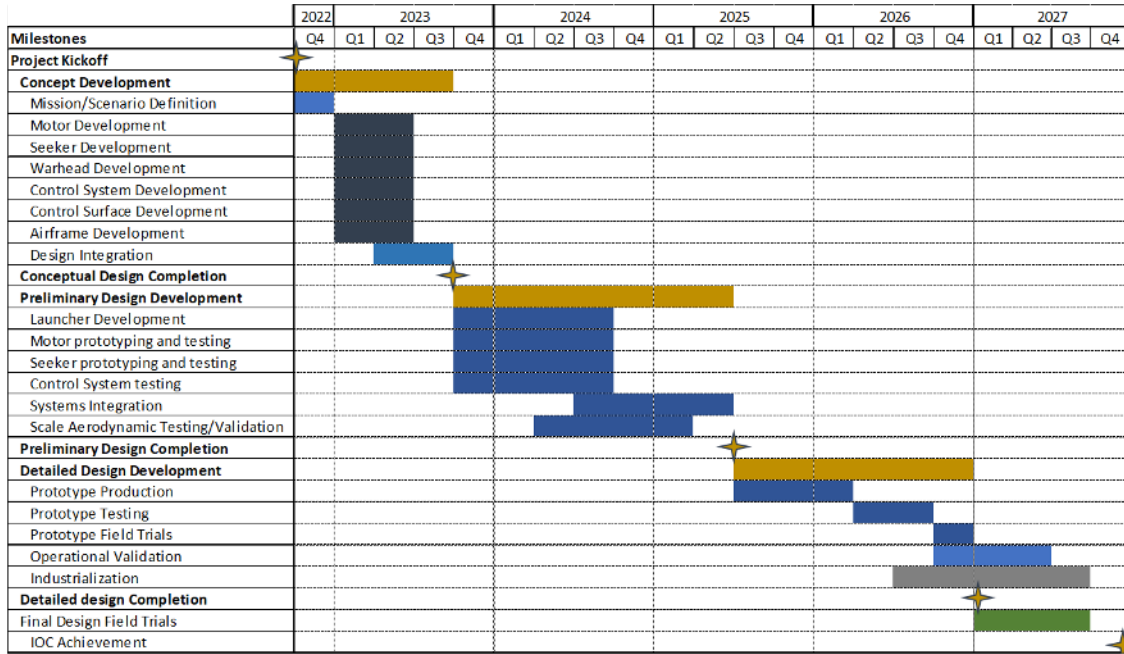
Figure 54: ISLAND Development Plant

6.10.3   Life Cycle Cost

The support costs for the ISLAND system are determined by calculating the per missile support costs from the Department of Defense Budget Estimates. Other options were investigated, but are limited by a lack of current data on modern systems. The Javelin Missile requires \$6,050 worth of support costs annually, and this is an appropriate and conservative estimate to apply to the ISLAND system [40]. Both systems are operated in small unit scenarios in active engagement, thus logistics, storage, and personal involvement would be similar. The costs can be considered conservative as the Javelin systems utilizes higher complexity thrust vectoring in its design. Applying the Javelin support cost value to the 2000 ISLAND missiles in the block, results in 12.1 million USD support costs per year, or a total operations cost for the 10 year life span of 121 million USD.

7 Conclusion

The ISLAND missile is a low-cost missile system that is specially designed to destroy Type 1 and Type 2 UAVs. It has a design range of 3.5 nautical miles and a design altitude of 5,000 feet. The system design, from the bottom up, was focused on user safety. Launch noise, acceleration and exhaust gases were all considered and mitigated. The ISLAND system's goal is to prevent asymmetric warfare. It achieves this goal with its low acquisition price of only $35,000. Further block upgrades to the ISLAND system can drive the price to below $25,000, similar in price to the Raytheon Coyote and $10,000 cheaper than the stinger missile.

This report shows the importance of incorporating launch safety early in the design. Novel and unconventional configurations must be evaluated in order to deliver a safe and effective design. Future work on the ISLAND will involve detailed aerodynamic stability analysis, further work into minimizing noise, and deeper trade studies with higher fidelity tools.

A compliance matrix, comparing the ISLAND performance to the AIAA RFP, is shown in Table 37.

Table 37: ISLAND compliance with the AIAA RFP requirements

Requirement	ISLAND Performance	Requirement Met	Analysis Location
"Threshold range of 3.0 nautical miles and an objective range of 3.5 nmi"	Design range: 3.5 nmi.	Yes, Objective	Section 6.7
"Threshold service ceiling of 3,000 ft AGL and an objective ceiling of 5,000 ft AGL"	Design altitude: 5,000 ft AG	Yes, Objective	Section 6.7
"Launcher + one missile shall weigh less than 40 pounds"	Missile Weight: 9.7 lb. Launcher weight: 25.4 lb,	Yes	Section 6.2, Section 6.8
"Launcher and 10 missiles must weigh no more than 125 pounds"	10 Missiles + Launcher Weight: 122 lb.	Yes	Section 6.2, Section 6.8
"The system must be capable operating in a raid scenario with up to 10 UAVs in an hour"	ISLAND reload and reengage performance: 2 minutes	Yes	Section 6.8
The system shall be compatible with safe storage, transportation, and handling requirements for at least 10 years without maintenance.	ISLAND propulsion system is capable of 10-year storage	Yes	Section 6.6
A warhead shall not be armed within 200 ft of the launch location.	Programmable proximity fuse guarantees safe arming distance	Yes	Section 6.9
The decibel noise level shall not exceed 120dBA within 100ft of the launch location.	Launch Noise: 151 dBA 100ft Noise: 117 dBA	No, see analysis	Section 5.3.3, Section 6.9
The missile shall not accelerate more than 2g's at launch	Launch Acceleration: 2g's due ejectable soft launch	Yes	Section 6.9
System initial operational capability (IOC) shall occur no later than December 2027.	Expected IOC: Q4 2027	Yes	Section 6.10

8 Acknowledgements

References

[1] Markets and Markets. *Small Drones Market Size, Growth, Trend and Forecast to 2025*. 2017. URL: `https://www.marketsandmarkets.com/Market-Reports/small-uav-market-141134567.html`.

[2] Joseph J Beel. "Anti-UAV Defense Requirements for Ground Forces and Hypervelocity Rocket Lethality Models". PhD thesis. Naval Postgraduate School, 1992.

[3] Edward A. Guelfi. "The Imperative for the U.S. Military to Develop a CounterUAS Strategy". In: (2020). URL: `https://ndupress.ndu.edu/Portals/68/Documents/jfq/jfq-97/jfq-97_4-12_Guelfi-Jayamaha-Robison.pdf?ver=2020-03-31-113800-930`.

[4] Jacob Gleason and Mark Vermylen. *Unmanned Aircraft System (UAS) Basics*. 2017. URL: `https://missile%20defenseadvocacy.org/missile-threat-and-proliferation/missile-basics/unmanned-aircraft-systems-uas/`.

[5] Paul Fahlstrom and Thomas Gleason. *Introduction to UAV Systems*. 4th. Wiley, 2012.

[6] Tim Weilkiens. *Systems Engineering with SysML/UML*. Morgan Kaufmann, 2007.

[7] AIAA. "Graduate Team Missile Systems Design Competition – Shoulder-Launched Anti- UAV Missile System". In: (2020). URL: `https://www.aiaa.org/docs/default-source/uploadedfiles/membership-and-communities/university-students/design-competitions/aiaa-2021-graduate-team-missile-design_competition-rfp.pdf?sfvrsn=c6c3ad23_0`.

[8] Paul Zarchan. *Ballistic Missile Defense Guidance and Control Issues*. Science & Global Security, 1998.

[9] John Boyd, et Al. "Energy Maneuverability (U)". In: (1966). URL: `https://www.archives.gov/files/declassification/iscap/pdf/2011-052-doc1.pdf`.

[10] J. Howell. "LAAD Evolves to Counter Modern Threats". In: (2019). URL: `https://www.marines.mil/News/News-Display/Article/1798431/laad-evolves-to-counter-modern-threats/`.

[11] Department of the Army. "JAVELIN—CLOSE COMBAT MISSILE SYSTEM, MEDIUM ". In: (2008). URL: `https://fas.org/irp/doddir/army/fm3-22-37.pdf`.

[12] Raytheon Technologies company. "What We Do - Defense". In: (2021). URL: `https://www.rtx.com/our-company/what-we-do/defense`.

[13] John B. Nowell. "Missile Total and Subsection Weight and Size Estimation Equations". In: (1984). URL: `https://apps.dtic.mil/dtic/tr/fulltext/u2/a256081.pdf`.

[14] Ronald Humble. *Space Propulsion Analysis and Design*. 1st. McGraw-Hill, 2007.

[15] Eugene L. Fleeman. *Tactical Missile Design*. 1st. AIAA, 2001.

[16] Wilson, R. C. *Development and Validation of a Solid Rocket Motor Analysis Code*. Georgia Institute of Technology, 2019.

[17] Philip Hill and Carl Peterson. *Mechanics and Thermodynamics of Propulsion*. 2010. DOI: `10.1017/cbo9781316106167.005`.

[18] Erik Cheever. "Fourth Order Runge-Kutta". In: (2021). URL: `https://lpsa.swarthmore.edu/NumInt/NumIntFourth.html`.

[19] Viswanath Devan. "Lie Algebra Application to Proportional Navigation Guidance of Missile". In: (2015). URL: `DOI:%2010.13140/2.1.2850.6402`.

[20] Rockwell Collins. "NavStrike Data Sheet". In: (2019). URL: `https://www.rockwellcollins.com/m/-/media/Files/Uns%20ecure/Products/Product_Brochures/Navigation_and_Guidance/GPS_Devices/NavStrike_data_sheet.ashx`.

[21] HENAN ZHENGZHOU. "Radar Drone Detection". In: (2020). URL: `https://www.antidrone-system.com/radar-drone-detection.html`.

[22] R. Zaeim, M.A. Nekoui, and A. Zaeim. "Integration of imaging seeker control in a visually guided missile". In: *IEEE ICCA 2010*. 2010, pp. 46–51. DOI: `10.1109/ICCA.2010.5524418`.

[23] NMCPHC. "Industrial Hygiene Field Operations Manual". In: (2021). URL: `https://www.med.navy.mil/sites/nmcphc/Documents/industrial-hygiene/IHFOM_CH5.pdf`.

[24] USAPHC. "Readiness through Hearing Loss Prevention". In: (2014). URL: `https://phc.amedd.army.mil/phc%5C%20resource%5C%20library/tg250.pdf`.

[25] Jeff Greason. "Rocket sound levels". In: (2000). URL: `https://ipfs.io/ipfs/QmdA5Wk%20DNALetBn4%20iFeSepHjdLGJdxPBwZyY47ir1bZGAK/space/rocket/rocket_noise.html`.

[26] SAS Institute Inc. "JMP". In: (2021). URL: `https://www.jmp.com/en_us/home.html`.

[27] Apogee Rockets. "CESARONI - P29-1G VMAX (F120)". In: (2021). URL: `https://www.apogeerockets.com/Rocket_Motors/Cesaroni_Prope%20llant_Kits/29mm_Motors/1_Grain_Motors%20/Cesaroni_P29-1G_Vmax_F120`.

[28] ESTES. " D12-3 ENGINES". In: (2021). URL: https://www.google.com/search?q=Estes+D12&oq=estes&aqs=chrome.0.69i59j46i199i275i291i433j35i39j0i131i433j69i60l4.945j0j9&sourceid=chrome&ie=UTF-8.

[29] Gerald Chaikin. " Predicting Peak Pressure Levels of Shoulder-Launched Rockets and Missiles". In: (1977). URL: https://apps.dtic.mil/sti/citations/ADA041333.

[30] U.S. Department of Defense. "MIL-STD-1474E: Design Criteria Standard Noise Limits". In: April (1997), pp. 1–219.

[31] CRAFT Tech. "Jet Noise Reduction - CRAFT Tech". In: (2020). URL: http://www.craft-tech.com/applications/acoustics/jet-noise-reduction/.

[32] R. H. Schlinker. " Supersonic Jet Noise from Round and Chevron Nozzles: Experimental Studies ". In: (2009). URL: https://colonius.caltech.edu/pdfs/SchlinkerSimonichShannonEtAl2009.pdf.

[33] Engineering Sound Solutions. *Technical Data Sheets _ Polymer Technologies Inc*. 2021. URL: https://www2.polytechinc.com/tds.

[34] Mark Bannon and Frank Kaputa. *Calculating Noise Reduction Coefficients & Decibel Drop*. 2015. URL: https://www.thermaxxjackets.com/noise-reduction-coefficients-and-decibel-drop/.

[35] I. Herrero-Durá, et Al. "Sound Absorption and Diffusion by 2D Arrays of Helmholtz Resonators. Applied Sciences". In: (2020). URL: https://doi.org/10.3390/app10051690.

[36] NATO Research and Technology Organisation Task Group HFM-147. *Hearing Protection – Needs , Technologies and Performance*. Vol. 323. November. 2010. ISBN: 9789283701217.

[37] Raytheon Missiles & Defense. *Coyote UAS*. 2020. URL: https://www.raytheonmissiles%20anddefense.com/%20capabilities/products/coyote.

[38] FAS. "Damage Criteria". In: (2021). URL: https://fas.org/man/dod-101/navy/docs/es310/dam_crit/dam_crit.htm.

[39] Robert E. Ball. *The Fundamentals of Aircraft Combat Survivability Analysis and Design*. 2nd. AIAA, 2003.

[40] Department of Defense. "Department of Defense Fiscal Year (FY) 2019 Budget Estimates". In: (2018). URL: https://www.asafm.army.mil/%20Portals/72/Documents/BudgetMaterial%20/2019/Base%5C%20Budget/Justification%20%5C%20Book/Missiles.pdf.

Nomenclature

Section 4.2 Weights, Structures, and Cost

ρ_{casing}	Casing density		$m_{igniter}$	Igniter mass
$\rho_{propellant}$	Propellant density		$m_{insulation}$	Insulation mass
σ	Yield stress		$m_{missile}$	Total missile mass
A_{wall}	Wall area		$m_{propellant}$	Propellant mass
C_{1000}	Unit production cost of 1000th missile		m_{nozzle}	Nozzle mass
C_{SDD}	System design and development cost		$m_{subsystems}$	Subsystem mass
D	Drag		$m_{surfaces}$	Surfaces mass
d	Average diameter		$m_{warhead}$	Warhead mass
d_{casing}	Casing diameter		$n_{surfaces}$	Number of surfaces
$d_{missile}$	Missile diameter		p_{int}	Internal pressure
E	Modulus of Elasticity		R	Design range
L	Lift		r	Radius
$L_{missile}$	Missile length		$S_{surfaces}$	Surface Area
$t_{bending}$	Bending thickness		V_c	Cavity Volume volume
$t_{buckling,bending}$	Buckling, bending thickness		V_{casing}	Casing volume
$t_{buckling,compression}$	Buckling, compression thickness		V_{GNC}	GNC volume
t_{burn}	Burn time		$V_{propellant}$	Propellant volume
$t_{insulation}$	Insulation thickness		$V_{subsystem}$	Subsystem volume
$t_{overall}$	Overall Thickness		$V_{surfaces}$	Surfaces volume
$t_{pressure}$	Pressure Thickness		$V_{warhead}$	Warhead volume
t_{SDD}	Program development time		W_L	Missile Launch Weight
$t_{surfaces}$	Surface thickness			
t_{thrust}	Thickness Thrust			
t_{mfg}	Thickness Manufacturing			
M	Mach Number			
m_{casing}	Casing mass			
m_{GNC}	Guidance, Navigation and Control mass			

Section 4.4: Aerodynamics

α	Angle of attack	C_N	Normal force coefficient
δ	Surface deflection angle	$C_{N\alpha}$	Normal force curve slope
δ	Leading edge thickness angle	d	Diameter
Φ	Body incidence angle	l	Length
γ	Ratio of specific heats	n_W	Number of surfaces
Λ	Leading edge sweep angle	M	Mach
a	Body cross section major axis	q	Dynamic pressure
A_e	Nozzle exit area	S_{Hemi}	Hemisphere reference area
b	Span	S_{Ref}	Reference area
b	Body cross section minor axis	S_W	Surface area
C_A	Axial force coefficient	t_{MAC}	Thickness at the mean aerodynamic chord
C_D	Drag coefficient	x_{AC}	Aerodynamic center location
C_{D0}	Zero lift drag coefficient	x_{CG}	Center of gravity location
C_L	Lift coefficient	x_{CP}	Center of pressure location
c_{mac}	Mean aerodynamic chord		

Subscripts

B	Body
W	Wing
N	Nose
T	Tail
LE	Leading edge
AC	Aerodynamic center
CG	Center of gravity
CP	Center of pressure
MAC	Mean aerodynamic center

Section 4.5: Trajectory

α	Angle of attack
γ	Flight path angle
θ	Pitch angle
ρ	Air density
λ	Line of sight angle
σ	Noise standard deviation
A	State transition matrix
a	Temperature Slope
a_{max}	Max acceleration
D	Drag
F_x	Horizontal force
F_y	Vertical force
g	Gravity
h	Altitude
H	Measurement Matrix
K	Gain
K_p	Proportional Gain
L	Lift
m	Mass
P	Covariance matrix
q	Pitch rate
Q	Process noise matrix
R	Measurement noise matrix
T	Thrust
t	Time
v_x	Horizontal velocity
v_y	Vertical velocity
W	Weight

ISLAND

x	Horizontal distance
v	Velocity
y	Vertical distance

Subscripts

0	Condition at 0 ft
opt	Optimal condition
t	Target
m	Missile
k	Current Step

Section 4.6.1: and Section 5.3.3: Launch Safety - Noise

θ	Pitch Angle
a	Acceleration
C	Sound-reduction coefficient
D	Missile diameter
d	Decibel drop
I_{sp}	Specific impulse
L	Launch tube length
$m_{missile}$	Missile mass
P_p	Peak pressure
R	Distance to noise source
V	Launch velocity
W	Missile weight

Section 4.6.2 and Section 5.3.2: Launch Safety - Acceleration

θ_{launch}	Launch angle	t_{tube}	Travel time within tube
a_{launch}	Launch acceleration	V_{exit}	Exit velocity
F_{net}	Net force		
$m_{missile}$	Missile mass		
T	Thrust		

Appendix

SECTION A-A

Ø1.40
1.26
0.28
4.00
21.21
28.31
Ø2.34
2.04

SECTION E-E
SCALE 1 : 2
25°
Quarter Chord

SECTION D-D
SCALE 1 : 2
25°
Quarter Chord

DETAIL C
SCALE 1 : 2
1.37
1.80
8°
0.72
0.20

DETAIL B
SCALE 1 : 2
1.49
1.80
0.90
35°

All dimensions are in inches

SECTION A-A

4.50

0.85

0.85

19.40

48.00

13.48

18.48

Ø5.10

6.00

4.00

A

A

All dimensions are in inches